The Abdus Salam
International Centre for Theoretical Physics

United Nations
Educational, Scientific and
Cultural Organization

IAEA
International Atomic Energy Agency

2167-20

Advanced School on Direct and Inverse Problems of Seismology

27 September - 8 October, 2010

DIRECT AND INVERSE PROBLEMS IN GEODYNAMICS

Alik T. Ismail-Zadeh
Geophysical Institute, Karlsruhe Institute of Technology
Germany

IIEP
Moscow
Russia

and

Institut de Physique du Globe de Paris
France

Advanced School on Direct and Inverse Problems of Seismology

27 September 2010 - 9 October 2010

DIRECT AND INVERSE PROBLEMS IN GEODYNAMICS

Alik T. Ismail-Zadeh

Geophysical Institute, Karlsruhe Institute of Technology,
Hertzsrt. 16, Karlsruhe 76187, Germany

International Institute of Earthquake Prediction Theory and
Mathematical Geophysics, Russian Academy of Sciences,
84/32 Profsoyuznaya ul., Moscow 117997, Russia.

Institut de Physique du Globe de Paris,
1, rue Jussieu, 75238 Paris cedex 05.

MIRAMARE-TRIESTE
October 2010

1 Basic concepts of computational geodynamics

1.1 Introduction to scientific computing and computational geodynamics

Present life without computers is almost impossible: industry and agriculture, government and media, transportation and insurance are major users of computational power. The earliest and still principal users of computers are researchers who solve problems in science and engineering or more specifically, who obtain solutions of mathematical models that represent some physical situation. The methods, tools and theories required to obtain such solutions are together called *scientific computing*, and the use of these methods, tools and theories to resolve scientific problems is referred to as *computational science*. A majority of these methods, tools, and theories were developed in mathematics well before the advent of computers. This set of mathematical theories and methods is an essential part of numerical mathematics and constitutes a major part of scientific computing. The development of computers signalled a new era in the approach to the solution of scientific problems. Many of the numerical methods initially developed for the purpose of hand calculation had to be revised; new techniques for solving scientific problems using electronic computers were intensively developed. Programming languages, operating systems, management of large quantities of data, correctness of numerical codes and many other considerations relevant to the efficient and accurate solution of the problems using a large computer system became subjects of the new discipline of computer science, on which scientific computing now depends heavily. Mathematics itself continues to play a major role in scientific computing: it provides the information about the suitability of a model and the theoretical foundation for the numerical methods.

There is now almost no area of science that does not use computers for modelling. In geosciences, meteorologists use parallel supercomputers to forecast weather and to predict the change of the Earth's climate; oceanographers use the power of computers to model oceanic tsunamis and to estimate harmful effects of the hazards on coastal regions; solid Earth physicists employ computers to study the Earth's deep interior and its dynamics. The planet Earth is a complex dynamical system. To gain a better understanding of the evolution of our planet, several concepts from various scientific fields and from mathematics should be combined in computational models. Great advances in understanding the Earth as well as in experimental techniques and in computational tools are transforming geoscience in general and geodynamics particularly.

Modern geodynamics was born in the late 1960s with the general acceptance of the plate tectonics paradigm. At the beginning, simple analytical models were developed to

explain plate tectonics and its associated geological structures. These models were highly successful in accounting for many of the first order behaviours of the Earth. The necessity to go beyond these basic models to make them more realistic and to understand better the Earth shifted the emphasis to numerical simulations. These numerical models have grown increasingly complex and capable over time with improvements in computational power and numerical algorithms. This has resulted in the development of a new branch of geoscience: *computational geodynamics*.

Characteristic of this new intellectual landscape is the need for strong interaction across traditional disciplinary boundaries: *geodynamics*, *mathematics* and *computer science*. Computational geodynamics can be defined as a blending of these three areas to obtain a better understanding of some phenomena through a match between the problem, computer architecture and algorithms. The computational approach to geodynamics is inherently *multi-disciplinary.* Mathematics provides the means to establish the credibility of numerical methods and algorithms, such as error analysis, exact solutions, uniqueness and stability analysis. Computer science provides the tools, ranging from networking and visualisation tools to algorithms matching modern computer architectures.

1.2 Mathematical models of geodynamic problems

Many geodynamic problems can be described by mathematical models, i.e. by a set of partial differential equations and boundary and/or initial conditions defined in a specific domain. Models in computational geodynamics predict quantitatively what will happen when the crust and the mantle deform slowly over geological time, often with the complications of simultaneous heat transport (e.g. thermal convection in the mantle), phase changes in the deep interior of the Earth, complex rheology (e.g. non-Newtonian flow, elasticity and plasticity), melting and melt migration, chemical reactions (e.g. thermo-chemical convection), solid body motion (e.g. idealised continent over the mantle), lateral forces, etc.

A mathematical model links the causal characteristics of a geodynamic process with its effects. The causal characteristics of the modelled process include, for example, parameters of the initial and boundary conditions, coefficients of the differential equations, and geometrical parameters of a model domain. The aim of the *direct* (sometimes called *forward*) mathematical problem is to determine the relationship between the causes and effects of the geophysical process and hence to find a solution to the mathematical problem for a given set of parameters and coefficients.

An *inverse* mathematical problem is the opposite of a direct problem. An inverse problem is considered when there is a lack of information on the causal characteristics (but information on the effects of the geophysical process exists). Inverse problems can be subdivided into time-reverse problems (e.g. to restore the development of a geodynamic process), coefficient problems (e.g. to determine the coefficients of the model equations and/or boundary conditions), geometrical problems (e.g. to determine the location of heat sources in a model domain or the geometry of the model boundary), and some others.

Inverse problems are often ill-posed. Jacques Hadamard, a French mathematician, introduced the idea of well- (and ill-) posed problems in the theory of partial differential equations (Hadamard, 1902). A mathematical model for a geophysical problem has to be *well-posed* in the sense that it has to have the properties of (1) existence, (2) uniqueness and (3) stability of a solution to the problem. Problems for which at least one of these properties does not hold are called *ill-posed*. The requirement of stability is the most important one. If a problem lacks the property of stability then its solution is almost impossible to compute because computations are polluted by unavoidable errors. If the solution of a problem does not depend continuously on the initial data, then, in general, the computed solution may have nothing to do with the true solution. We should note that despite the fact that many inverse problems are ill-posed, there are methods for solving the problems (see, for example, Tikhonov and Arsenin, 1977). While most geodynamic models are concerned with direct (forward) problems, there is increasing interest in the inverse problem (or data assimilation), as discussed in Chapter 8.

1.3 Governing equations

In this section we present the basic equations that govern geodynamic processes. The equations are partial differential equations (PDEs), involving more than one independent variable. PDEs can be distinguished by the following property. Consider a partial differential equation in the following form: $A\Psi_{xx} + B\Psi_{xy} + C\Psi_{yy} = f(x, y, \Psi, \Psi_x, \Psi_y)$, where A, B and C are constants. Depending on $D = B^2 - 4AC$, a PDE is called *elliptic* if $D < 0$, *parabolic* if $D = 0$ or *hyperbolic* if $D > 0$. Examples of these in solid Earth dynamics are the solution of gravitational potential (elliptic), thermal diffusion (parabolic) and seismic wave propagation (hyperbolic).

Because the mantle behaves basically as a viscous fluid for the geological time scale, the governing equations describe the flow of highly viscous fluid. The basic conservation laws used to derive these equations are only briefly summarised (see Chandrasekhar, 1961, and Schubert *et al*., 2001, for details).

1.3.1 The equation of continuity

Consider a fluid in which the density ρ is a function of position x_j ($j = 1, 2, 3$ hereinafter). Let u_j denote the components of the velocity. We shall use the notation of Cartesian tensors with the usual summation convention. Consider the physical law of the *conservation of mass*: the rate of change of the mass contained in a fixed volume V of the fluid is given by the rate at which the fluid flows out of it across the boundary S of the volume. Mathematically it is expressed as

$$\frac{\partial}{\partial t}\int_V \rho d\tau = -\int_S \rho u_j dS_j, \tag{1.1}$$

where τ is the volume element. The use of the Gauss–Ostrogradsky (divergence) theorem transforms the law of mass conservation into the following equation

$$\frac{\partial}{\partial t}\int\limits_V \rho d\tau = -\int\limits_V \frac{\partial}{\partial x_j}(\rho u_j)d\tau. \tag{1.2}$$

An alternative form of the equation, which is useful for numerical analysis is the Lagrangian continuity equation:

$$\frac{D\rho}{Dt} \equiv \frac{\partial \rho}{\partial t} + u_j\frac{\partial \rho}{\partial x_j} = -\rho\frac{\partial u_j}{\partial x_j}, \tag{1.3}$$

which can also be written in Eulerian form:

$$\frac{\partial \rho}{\partial t} = -\frac{\partial}{\partial x_j}(\rho u_j). \tag{1.4}$$

For an incompressible fluid, the equation of continuity reduces to:

$$\frac{\partial u_j}{\partial x_j} = 0, \text{ because } \frac{\partial \rho}{\partial t} + u_j\frac{\partial \rho}{\partial x_j} = \frac{D\rho}{Dt} = 0. \tag{1.5}$$

1.3.2 The equation of motion

Consider the physical law of the *conservation of momentum*: the rate of change of the momentum contained in a fixed volume V of the fluid is equal to the volume integral of the external body forces acting on the elements of the fluid plus the surface integral of normal and shear stresses acting on the bounding surface S of the volume V minus the rate at which momentum flows out of the volume across the boundaries of V by the motions prevailing on the surface S. Mathematically it is expressed as

$$\frac{\partial}{\partial t}\int\limits_V \rho u_i d\tau = \int\limits_V \rho F_i d\tau + \int\limits_S \sigma_{ij} dS_j - \int\limits_S \rho u_i u_j dS_j, \tag{1.6}$$

where F_i $(= g_i)$ is the ith component of external (usually gravity) force per unit of mass; and σ_{ij} is the stress tensor. We note that

$$\frac{\partial}{\partial t}(\rho u_i) = \rho\frac{\partial u_i}{\partial t} + u_i\frac{\partial \rho}{\partial t} = \rho\frac{\partial u_i}{\partial t} - u_i\frac{\partial}{\partial x_j}(\rho u_j). \tag{1.7}$$

If we substitute now expression (1.7) into (1.6), we obtain

$$\int\limits_V \left(\rho\frac{\partial u_i}{\partial t} - u_i\frac{\partial}{\partial x_j}(\rho u_j)\right)d\tau + \int\limits_S \rho u_i u_j dS_j = \int\limits_V \rho F_i d\tau + \int\limits_S \sigma_{ij} dS_j. \tag{1.8}$$

Integrating by parts the second term of the first volume integral, we obtain

$$-\int_V u_i \frac{\partial}{\partial x_j}(\rho u_j) d\tau + \int_S \rho u_i u_j dS_j = \int_V \rho u_j \frac{\partial u_i}{\partial x_j} d\tau. \tag{1.9}$$

Application of the Gauss–Ostrogradsky theorem to the last term in (1.8) gives:

$$\int_S \sigma_{ij} dS_j = \int_V \frac{\partial \sigma_{ij}}{\partial x_j} d\tau. \tag{1.10}$$

Substituting Eqs. (1.9) and (1.10) in (1.8) we obtain the *equation of motion* which is valid for any arbitrary volume V

$$\rho \frac{\partial u_i}{\partial t} + \rho u_j \frac{\partial u_i}{\partial x_j} = \rho F_i + \frac{\partial \sigma_{ij}}{\partial x_j}. \tag{1.11}$$

For linear viscous creep, the stress is related to the rate of increase of strain (strain rate) as

$$\begin{aligned} \sigma_{ij} &= -P\delta_{ij} + 2\eta \dot{\varepsilon}_{ij} + \left(\eta_B - \frac{2}{3}\eta\right) \delta_{ij} \frac{\partial u_k}{\partial x_k} \\ &= -P\delta_{ij} + \eta \left(\frac{\partial u_i}{\partial x_j} + \frac{\partial u_j}{\partial x_i} - \frac{2}{3}\delta_{ij} \frac{\partial u_k}{\partial x_k} \right) + \eta_B \delta_{ij} \frac{\partial u_k}{\partial x_k}, \end{aligned} \tag{1.12}$$

where P is the pressure, δ_{ij} is the Kronecker delta, η is the viscosity, η_B is the bulk viscosity, and $\dot{\varepsilon}_{ij}$ is the strain rate tensor. As compaction or dilation is normally accommodated elastically, η_B is usually assumed to be zero. By substituting the relationship (1.12) into the equation of motion (1.11) and assuming $\eta_B = 0$, we obtain

$$\rho \frac{\partial u_i}{\partial t} + \rho u_j \frac{\partial u_i}{\partial x_j} = \rho F_i - \frac{\partial P}{\partial x_i} + \frac{\partial}{\partial x_j} \left\{ \eta \left(\frac{\partial u_i}{\partial x_j} + \frac{\partial u_j}{\partial x_i} - \frac{2}{3}\delta_{ij} \frac{\partial u_k}{\partial x_k} \right) \right\}. \tag{1.13}$$

For an incompressible, constant-viscosity fluid, equation (1.13) simplifies to

$$\rho \frac{\partial u_i}{\partial t} + \rho u_j \frac{\partial u_i}{\partial x_j} = \rho F_i - \frac{\partial P}{\partial x_i} + \eta \nabla^2 u_i. \tag{1.14}$$

Equation (1.14) represents the original form of the *Navier–Stokes* equations.

Now we show that in geodynamical applications the Navier–Stokes equations (1.14) are transformed into the Stokes equations. Let us define new dimensionless variables and parameters (denoted by a tilde) as $t = \tilde{t} l_* / \kappa_*$, $\mathbf{x} = \tilde{\mathbf{x}} l_*$, $\mathbf{u} = \tilde{\mathbf{u}} \kappa_* / l_*$, $P = \tilde{P} \eta_* \kappa_* / l_*^2$, $\rho = \tilde{\rho} \rho_*$, and $\eta = \tilde{\eta} \eta_*$, where $\rho_* = 4 \times 10^3$ kg m^{-3}, $\eta_* = 10^{21}$ Pa s, $l_* = 3 \times 10^6$ m, and $\kappa_* = 10^{-6}$ m^2 s^{-1} are typical values of the density, viscosity, length and thermal diffusivity for the Earth's mantle, respectively. We assume that $F_i = (0, 0, g)$, where $g = 9.8$ m s^{-2} is the acceleration due to gravity. After the replacement of the variables by their dimensionless form (and omitting tildes), we obtain:

$$\frac{1}{Pr} \rho \left(\frac{\partial u_i}{\partial t} + u_j \frac{\partial u_i}{\partial x_j} \right) = -\frac{\partial P}{\partial x_i} + \frac{\partial}{\partial x_j} \left\{ \eta \left(\frac{\partial u_i}{\partial x_j} + \frac{\partial u_j}{\partial x_i} - \frac{2}{3}\delta_{ij} \frac{\partial u_k}{\partial x_k} \right) \right\} + La\, \rho \delta_{i3}, \tag{1.15}$$

where the dimensionless parameter $Pr = \frac{\eta_*}{\rho_* \kappa_*} = 2.5 \times 10^{23}$ is the Prandtl number; and the dimensionless parameter $La = \frac{\rho_* g l_*^3}{\eta_* \kappa_*} \sim 10^9$ is the Laplace number. Note that $La = Ra/(\alpha \Delta T)$, where Ra is the Rayleigh number controlling the vigour of thermal convection, α is the thermal expansivity and ΔT is the typical temperature variation. Therefore, (1.15) are reduced to the following elliptic equations called the *Stokes equations*:

$$0 = -\frac{\partial P}{\partial x_i} + \frac{\partial}{\partial x_j}\left\{\eta\left(\frac{\partial u_i}{\partial x_j} + \frac{\partial u_j}{\partial x_i} - \frac{2}{3}\delta_{ij}\frac{\partial u_k}{\partial x_k}\right)\right\} + \frac{Ra}{\alpha \Delta T}\rho \delta_{i3} \tag{1.16}$$

or, in dimensional units,

$$0 = -\frac{\partial P}{\partial x_i} + \frac{\partial}{\partial x_j}\left\{\eta\left(\frac{\partial u_i}{\partial x_j} + \frac{\partial u_j}{\partial x_i} - \frac{2}{3}\delta_{ij}\frac{\partial u_k}{\partial x_k}\right)\right\} + \rho F_i. \tag{1.17}$$

For incompressible flow the $-\frac{2}{3}\delta_{ij}\frac{\partial u_k}{\partial x_k}$ term is omitted. For constant viscosity and incompressible flow the second term reduces to $\eta \nabla^2 u_i$ as in Eq. (1.14).

1.3.3 The heat equation

Consider the physical law of the *conservation of energy*. Counting the gains and losses of energy that occur in a volume V of the fluid, per unit time, we have

$$\frac{\partial}{\partial t}\int_V \rho E d\tau = \int_S u_i \sigma_{ij} dS_j + \int_V \rho u_i F_i d\tau - \int_S k\frac{\partial T}{\partial x_j} dS_j - \int_S \rho E u_j dS_j + \int_V \rho H d\tau. \tag{1.18}$$

Here the first term of the right-hand side of the Eq. (1.18) is the rate at which work is done on the boundary; the second term represents the rate at which work is done on each element of the fluid inside V by the external forces; the third term is the rate at which energy in the form of heat is conducted across S; the fourth term is the rate at which energy is convected across S by the prevailing mass motion (k is the coefficient of heat conduction); and the fifth term is the rate at which energy is added by internal heat sources. The first and third terms of Eq. (1.18) can be represented as follows:

$$\int_S u_i \sigma_{ij} dS_j = \frac{1}{2}\frac{\partial}{\partial t}\int_V \rho u_i^2 d\tau + \frac{1}{2}\int_S \rho u_i^2 u_j dS_j - \int_V \rho u_i F_i d\tau + \int_V \Phi d\tau, \tag{1.19}$$

where $\Phi = \frac{\partial u_i}{\partial x_j}\sigma_{ij}$ is the viscous dissipation function, and

$$\int_S k\frac{\partial T}{\partial x_j} dS_j = \int_V \frac{\partial}{\partial x_j}\left(k\frac{\partial T}{\partial x_j}\right) d\tau. \tag{1.20}$$

The energy E per unit mass of the fluid can be written as

$$E = \frac{1}{2}u_i^2 + c_V T, \tag{1.21}$$

where c_V is the specific heat at constant volume and T is the temperature. This allows the fourth term of (1.16) to be rewritten as:

$$-\int_S \rho E u_j dS_j = -\int_S \rho \left[\frac{1}{2}u_i^2 + c_V T\right] u_j dS_j = -\frac{1}{2}\int_S \rho u_i^2 u_j dS_j - \int_V \frac{\partial}{\partial x_j}(\rho u_j c_V T) d\tau. \tag{1.22}$$

Substituting Eqs. (1.19)–(1.22) into (1.18), we obtain

$$\int_V \frac{\partial}{\partial t}(\rho c_V T) d\tau = \int_V \frac{\partial}{\partial x_j}\left(k\frac{\partial T}{\partial x_j}\right) d\tau + \int_V \Phi d\tau - \int_V \frac{\partial}{\partial x_j}(\rho c_V T u_j) d\tau + \int_V \rho H d\tau. \tag{1.23}$$

Since Eq. (1.23) is valid for any arbitrary volume V, we must have

$$\frac{\partial}{\partial t}(\rho c_V T) + \frac{\partial}{\partial x_j}(\rho c_V T u_j) = \frac{\partial}{\partial x_j}\left(k\frac{\partial T}{\partial x_j}\right) + \Phi + \rho H. \tag{1.24}$$

Noting that the left-hand side of the equation is the Lagrangian time derivative D/Dt, and applying the derivative separately to T and ρ results in:

$$\rho\frac{D}{Dt}(c_V T) + c_V T\frac{D\rho}{Dt} = \frac{\partial}{\partial x_j}\left(k\frac{\partial T}{\partial x_j}\right) + \Phi + \rho H, \tag{1.25}$$

which after some manipulation using thermodynamic expressions leads to the form

$$\rho c_p \frac{DT}{Dt} - \alpha T\frac{DP}{Dt} = \frac{\partial}{\partial x_i}\left(k\frac{\partial T}{\partial x_i}\right) + \Phi + \rho H. \tag{1.26}$$

This is a general form, valid for compressible flow. Various other forms exist. For example for incompressible flow, applying the incompressible continuity equation (1.5) to equation (1.24) results in the simplified form:

$$\rho\frac{\partial}{\partial t}(c_V T) + \rho u_j\frac{\partial}{\partial x_j}(c_V T) = \frac{\partial}{\partial x_j}\left(k\frac{\partial T}{\partial x_j}\right) + \Phi + \rho H. \tag{1.27}$$

We note that Eq. (1.27) is a parabolic equation. Equation (1.26) is often written using the ∇ operator as:

$$\rho c_p\left(\frac{\partial T}{\partial t} + \mathbf{u}\cdot\nabla T\right) - \alpha T\left(\frac{\partial P}{\partial t} + \mathbf{u}\cdot\nabla P\right) = \nabla\cdot(k\nabla T) + \Phi + \rho H. \tag{1.28}$$

1.3.4 The rheological law

In the mid twentieth century, E. C. Bingham introduced the term of 'rheology' in colloid chemistry, which has a meaning of 'everything flows' (in Greek $\pi\alpha\nu\tau\alpha\ \rho\varepsilon\iota$), the motto of the subject from Heraclitus (Reiner, 1964). A rheological law describes a relationship

between stress and strain (strain rate) in a material. We often hear that the Earth's mantle exhibits the rheological properties of a fluid or a solid. The Deborah number, a dimensionless number expressing the ratio between the time of relaxation and time of observation, can assist in the understanding of the behaviour of geomaterials. If the time of observation is very large (or the time of relaxation of the geomaterial under observation is very small), the mantle is considered to be a fluid and hence it flows. On the other hand, if the time of relaxation of the geomaterial is larger than the time of observation, the mantle is considered to be a solid. Therefore, the greater the Deborah number, the more solid the geomaterial (and vice versa, the smaller the Deborah number, the more fluid it is). In nature, geomaterials (e.g. rocks comprising the crust, lithosphere and mantle) exhibit more complicated rheological behaviour than fluid or solid materials. We consider here a few principal rheological relationships. For detailed information on rock rheology, the reader is referred to Ranalli (1995) and Karato (2008).

In geodynamic modelling a viscous rheology is extensively used, because the mantle behaves as a highly viscous fluid at geological time scales. The equation describing the relationship between the viscous stress and strain rate can be presented in the following form:

$$\tau_{ij} = C^{\frac{1}{n}} \dot{\varepsilon}_{ij} \dot{\varepsilon}^{\frac{1-n}{n}}, \tag{1.29}$$

where τ_{ij} is the deviatoric stress tensor, C is a proportionality factor defined from the thermodynamic conditions, $\dot{\varepsilon} = (0.5\dot{\varepsilon}_{kl}\dot{\varepsilon}_{kl})^{1/2}$ is the second invariant of the strain rate tensor, and n is a power-law exponent. If $n = 1$, Eq. (1.29) describes a *Newtonian fluid* with $C/2$ as the fluid's viscosity, which depends on temperature and pressure as discussed below. For $n > 1$, Eq. (1.29) represents a *non-Newtonian (non-linear) fluid*.

At high temperatures (that are a significant fraction of the melt temperature) the atoms and dislocations in a crystalline solid become sufficiently mobile to result in creep when the solid is subject to deviatoric stresses. At very low stresses diffusion processes dominate, and the crystalline solid behaves as a Newtonian fluid with a viscosity that depends exponentially on pressure and the inverse absolute temperature. The proportionality factor C in (1.29) can be then represented as:

$$C(T,P) = C^* d^m \exp\left(\frac{E + PV}{RT}\right), \tag{1.30}$$

where T is the absolute temperature, P is pressure, C^* is the proportionality factor that does not depend on temperature and pressure, E is the activation energy, V is the activation volume, R is the universal gas constant, and d is the grain size. For dislocation creep, grain size is unimportant and $m = 0$, but for diffusion creep m is between 2 and 3. At higher stresses the motion of dislocations becomes the dominant creep process resulting in a non-Newtonian fluid behaviour described by Eqs. (1.29)–(1.30), with typically $n = 3.5$. Thermal convection in the mantle and some aspects of lithosphere dynamics are attributed to these thermally activated creep processes. The temperature–pressure dependence of the rheology of geomaterials is important in understanding the role of convection in transporting heat.

During dislocation creep as mentioned above, diffusion-controlled climb of edge dislocations is the limiting process. At low temperatures this is extremely slow, but can be

bypassed at stresses high enough to force dislocations through obstacles, a process known as low-temperature (Peierls) plasticity. In this case, the exponential proportionality factor C becomes stress-dependent. A commonly assumed form of the strain rate dependence on stress is:

$$\dot{\varepsilon} = A \exp\left[-\frac{H_0}{RT}\left(1 - \frac{\sigma}{\sigma_P}\right)^2\right], \tag{1.31}$$

where σ_P is the Peierls stress, which is of order 2–9 GPa, and σ is the second invariant of the stress tensor.

Creep processes can relax elastic stresses in the lower lithosphere. Such behaviour can be modelled with a rheological law that combines linear elasticity and linear or non-linear viscosity. A material that behaves elastically on short time scales and viscously on long time scales, is referred to as a viscoelastic material. The most commonly employed rheology to simulate numerically lithosphere dynamics is the *viscoelastic* (*Maxwell*) rheology. According to the Hooke law of elasticity, the elastic strain ε_{ij} and the deviatoric stress τ_{ij} are related as

$$\tau_{ij} = \mu \varepsilon_{ij}, \tag{1.32}$$

where μ is the shear modulus. For the fluid we assume a linear Newtonian relation between viscous strain rate and the stress (consider Eq. (1.29) with $n = 1$ and $C = 2\eta$)

$$\tau_{ij} = 2\eta \frac{\partial \varepsilon_{ij}}{\partial t}, \tag{1.33}$$

where η is the fluid viscosity. The Maxwell model for a viscoelastic geomaterial assumes that the strain rate of the geomaterial is a superposition of the elastic and viscous strain rates, namely,

$$\frac{\partial \varepsilon_{ij}}{\partial t} = \frac{\tau_{ij}}{2\eta} + \frac{1}{\mu}\frac{\partial \tau_{ij}}{\partial t} \quad \text{or} \quad \left(1 + 2t_r \frac{\partial}{\partial t}\right)\tau_{ij} = 2\eta \frac{\partial \varepsilon_{ij}}{\partial t}, \tag{1.34}$$

where $t_r = \eta/\mu$ is the viscoelastic relaxation (or Maxwell relaxation) time. We see that on time scales short compared with the time of relaxation t_r the geomaterial behaves elastically, and on time scales long compared with t_r the material behaves as a Newtonian fluid.

Because the effective viscosity of the shallow lithosphere is very high, its deformation is no longer controlled by dislocation creep; instead it is determined by (at lower pressures) the movement of blocks of the lithosphere along pre-existing faults of various orientations and (at higher pressures) deformation accommodated by distributed microcracking. The dynamic friction along such faults depends only weakly upon the strain rate, and is often idealised using the rheological model of a *perfectly plastic material*, which does not exhibit work-hardening but flows plastically under constant stress. Hence the stress–strain relationship for the lithosphere obeys the von Mises equations (Prager and Hodge, 1951)

$$\tau_{ij} = \kappa \dot{\varepsilon}_{ij}/\dot{\varepsilon}, \tag{1.35}$$

where κ is the yield limit. The second invariant of the stress, $\tau = (0.5\tau_{kl}\tau_{kl})^{1/2}$, equals the yield limit for any non-zero strain rate. When $\tau < \kappa$, there is no plastic deformation and hence no motion along the faults. A comparison of Eqs. (1.29) and (1.35) shows that the perfectly plastic rheology can be considered as the limit of non-Newtonian power-law rheology as $n \to \infty$ (and $C = \kappa$). In rocks, the yield stress κ depends on pressure. If κ increases linearly with pressure, as is commonly assumed, then this gives the *Drucker–Prager yield criterion*, $\kappa = a + bP$, where a and b are constants and P is the pressure.

Brittle failure may be treated by the *Mohr–Coulomb failure criterion*, which expresses a linear relationship between the shear stress and the normal stress resolved on the failure plane, which is oriented at a particular angle,

$$\tau_f = \sigma_f \tan\phi + c, \tag{1.36}$$

where τ_f and σ_f are the shear stress and normal stress acting on the failure plane, ϕ is the *angle of internal friction* and c is the *cohesion*. It is often more convenient to express this in terms of the maximum shear stress $\tau_{\max}$ and $\bar{\sigma}$, the average of the maximum and minimum principle stresses:

$$\tau_{\max} = \bar{\sigma}\sin\phi + c\cos\phi. \tag{1.37}$$

In numerical models the Mohr–Coulomb criterion is often approximated by the Drucker–Prager criterion, with $\tau_{\max}$ equal to the second stress invariant and pressure used in place of $\bar{\sigma}$.

Thus, a fluid behaviour of geomaterials is described by Eqs. (1.29)–(1.31), and (1.33), elastic behaviour by Eq. (1.32), viscoelastic by Eq. (1.34), perfectly plastic by Eq. (1.35) and brittle by Eq. (1.36)–(1.37). These relationships are used frequently in geodynamic modelling.

1.3.5 Other equations

The equations of continuity, motion and heat balance compose the basic equations governing models of mantle and lithosphere dynamics. Together with the basic equations, additional equations are necessary to describe the behaviour of mantle rocks, namely, equations of state, rheological law (or equation for viscosity), equation for phase transformations, etc. In many practical applications, a linear dependence of density on temperature (equation of state) is assumed:

$$\rho = \rho_0[1 - \alpha(T - T_0)], \tag{1.38}$$

where ρ_0 is a reference density, α is the coefficient of thermal expansivity and T_0 is a reference temperature. If phase transformations of mantle rocks are considered the state equation is modified. The viscosity of mantle rocks is the least well-known parameter used in numerical modelling of geodynamic problems. The mantle viscosity can depend on temperature, pressure, grain size, content of water or melt, stress, etc. We shall use various representations of viscosity in our geodynamic model examples (see Chapter 10).

1.3.6 Boussinesq approximation

Mantle dynamics is controlled by heat transfer, and the mantle properties are normally functions of temperature. The variations in density due to temperature variations are generally small and yet are the cause of the mantle motion. If the density variation is not large, one may treat the density as constant in the continuity equation (i.e. the fluid is assumed to be *incompressible* (Eq. 1.5)) and in the energy equation (e.g. in the unsteady and advection terms) and treat it as variable only in the gravitational (buoyancy) term of the momentum equation.

Consider the Stokes equation (1.17) and split the term $\rho F_i = \rho g_i$ into two parts: $\rho_0 g_i + (\rho - \rho_0) g_i$. The first part can be included with pressure and the density variation is retained in the gravitational term. The remaining term can be expressed as:

$$(\rho - \rho_0) g_i = -\rho_0 g_i \alpha (T - T_0). \tag{1.39}$$

Such simplification of the model is called the Boussinesq approximation. In the strict form of this, all physical properties except viscosity are constant. The dimensionless mass and energy conservation equations then become

$$-\frac{\partial P}{\partial x_i} + \frac{\partial}{\partial x_j}\left\{\eta\left(\frac{\partial u_i}{\partial x_j} + \frac{\partial u_j}{\partial x_i}\right)\right\} = RaT\delta_{i3}, \quad \frac{\partial T}{\partial t} + u_j \frac{\partial T}{\partial x_j} = \frac{\partial^2 T}{\partial x_j^2} + H. \tag{1.40}$$

If fluid is compressible, compressibility is incorporated in a model using either the *extended Boussinesq approximation*, in which the density is still assumed constant in the continuity equation but the extra terms are included in the energy equation, or the *anelastic approximation*, in which the density is assumed to vary with position but not with time. Both approximations are discussed in detail in Section 10.3.

1.3.7 Stream function formulation

The stream function formulation is a way of eliminating pressure and reducing two velocity components to a single scalar, in two-dimensional geometry. The velocity field $\mathbf{v} = (u_1, u_3)$ in two dimensions (x_1, x_3) is related to derivatives of a scalar stream function ψ:

$$\mathbf{v} = \left(\frac{\partial \psi}{\partial x_3}, -\frac{\partial \psi}{\partial x_1}\right). \tag{1.41}$$

Often, the opposite sign is used. It is easily verified that this satisfies the incompressible continuity equation (Eq. 1.5). Substituting this into the constant-viscosity Boussinesq Stokes equation for thermally driven flow,

$$-\nabla P + \nabla^2 \mathbf{v} = RaT\mathbf{e}, \tag{1.42}$$

where $\mathbf{e}$ is the unit vector, and taking the out of plane (y) component of the curl of this equation yields:

$$\nabla^4 \psi = -Ra \frac{\partial T}{\partial x_1}. \tag{1.43}$$

Hence, three variables (two velocity components and pressure) have been reduced to one scalar. This can be solved as a fourth-order differential equation, or split into two second-order equations:

$$\nabla^2\omega = -Ra\frac{\partial T}{\partial x_1}, \quad \nabla^2\psi = \omega, \tag{1.44}$$

where ω is the vorticity, which is the out of plane (y) component of $\nabla \times \mathbf{v}$. This formulation can also be used to re-express the variable-viscosity Stokes equation, but a more complicated expression results (see Malevsky and Yuen, 1992).

1.3.8 Poloidal and toroidal decomposition

A way of simplifying the Stokes and continuity equations in three dimensions is to express the velocity field in terms of poloidal and toroidal mass flux potentials:

$$\rho\mathbf{v} = \nabla \times \nabla \times (W\mathbf{e}) + \nabla \times (Z\mathbf{e}), \tag{1.45}$$

where $\mathbf{v} = (u_1, u_2, u_3)$ is the velocity field, W is the poloidal potential, and Z is the toroidal potential. This automatically satisfies the continuity equation, which is therefore eliminated, and reduces the three velocity components to two scalars. If the flow is incompressible, then W and Z become velocity potentials:

$$\mathbf{v} = \nabla \times \nabla \times (W\mathbf{e}) + \nabla \times (Z\mathbf{e}). \tag{1.46}$$

In the case of homogeneous boundary conditions and viscosity that does not vary in the horizontal directions, there is no source for the toroidal term (see Ricard and Vigny, 1989), so this further reduces to

$$\mathbf{v} = \nabla \times \nabla \times (W\mathbf{e}). \tag{1.47}$$

Assuming constant properties and the Boussinesq approximation, by taking the x_3-component of the double curl of the momentum equation (1.42), substituting Eq. (1.47), and using identities such as $\nabla \times \nabla \times \mathbf{a} = \nabla(\nabla \cdot \mathbf{a}) - \nabla^2\mathbf{a}$, the Stokes equation can be reduced to the simple form:

$$\nabla^4 W = Ra\, T. \tag{1.48}$$

The pressure has been eliminated, so the number of variables has been reduced from four (pressure and three velocity components) to one. A poloidal–toroidal decomposition can also be used for flow in which viscosity varies (see Christensen and Harder, 1991) and/or the boundary conditions are not homogeneous (see Hager and O'Connell, 1981), but then the toroidal component must be retained and the resulting equations become much more complex.

1.4 Boundary and initial conditions

The equations given above govern the slow movements of the Earth's mantle and lithosphere. They are the same equations whether the movement is, for example, a thermal plume rising beneath a particular region, subduction of the lithosphere, a mid-ocean ridge, convective flow in the upper mantle or whole mantle convection. However, the movements are different for these cases, although the governing equations are the same. Why? If all parameters entering the governing equations are the same, the answer is because of the boundary and initial conditions, which are different for each of the above examples.

For example, rising mantle plumes require mainly free-slip conditions at the boundaries of a model domain. Meanwhile spreading at a mid-ocean ridge is driven partly by forces due to distant subduction, so for a local model of a mid-ocean ridge a velocity field should be imposed at the upper boundary of a model domain. The boundary and initial conditions dictate the particular solutions to be obtained from the governing equations. Therefore, once we have the governing equations, then the real driver for any particular solution is the boundary conditions.

Let us review the proper physical boundary conditions. When the condition on a surface of the Earth assumes zero relative velocity between the surface and the air immediately at the surface, we refer to the condition as the *no-slip* (or *rigid*) condition. If the surface is stationary, then

$$u_1 = u_2 = u_3 = 0. \tag{1.49}$$

When the velocity at the boundary is a finite, non-zero value and there is no mass flow in to or out of the model domain, the velocity vector immediately adjacent to the boundary must be tangential to this boundary. If $\mathbf{n}$ is a unit normal vector at a point on the boundary and $\mathbf{u}_\tau$ is the projection of the velocity vector onto the tangent plane at the same point on the boundary, the condition at this boundary can be given as

$$\mathbf{u} \cdot \mathbf{n} = 0, \quad \partial \mathbf{u}_\tau / \partial \mathbf{n} = 0. \tag{1.50}$$

These conditions are called *free-slip* conditions. The actual surface of the Earth can move upwards and downwards. The above conditions, in which the upper boundary of the model domain represents the Earth's surface and there is no vertical motion at the boundary, are idealisations made to simplify the model. Modelling an actual free surface that deflects vertically is more complicated but methods exist, as discussed in Chapter 10.

There is an analogous 'no-slip' condition associated with the temperature at the surface. If the temperature at the surface is denoted by T_u, then the temperature immediately in contact with the surface is also T_u. If in a given problem the temperature is known, then the proper condition on the temperature at the upper boundary of the model domain is

$$T = T_u. \tag{1.51}$$

On the other hand, if the temperature at the surface is not known, e.g. if it is changing with time due to heat transfer to the surface, then the Fourier law of heat conduction provides

the boundary condition at the surface. If we let $\dot{q}_u$ denote the instantaneous heat flux to the surface, then from the Fourier law

$$\dot{q}_u = -\left(k\frac{\partial T}{\partial n}\right)_u, \tag{1.52}$$

where n denotes the direction normal to the surface. The surface rocks are responding to the heat transfer to the surface, $\dot{q}_u$, hence changing T_u, which in turn affects $\dot{q}_u$. This general, unsteady heat transfer problem must be solved by treating the viscous flow and the thermal response of the surface rocks simultaneously. This type of boundary condition is a boundary condition on the temperature gradient at the surface, in contrast to stipulating the surface temperature itself as the boundary condition. That is, from Eq. (1.52),

$$\left(\frac{\partial T}{\partial n}\right)_u = -\frac{\dot{q}_u}{k}. \tag{1.53}$$

While the above discussion refers to the top boundary of the domain, similar conditions also apply to the lower boundary, which in global models is the core–mantle boundary. At the sides, no-slip or free-slip conditions are sometimes assumed, but if the model is intended to represent the entire mantle then periodic boundaries are most realistic. In local or regional models, which are often applied to model the crust and/or lithosphere, it is quite common for material to flow in or out of the domain, either with a prescribed velocity and temperature or with some other conditions such as prescribed normal stress, but we do not give mathematical details here.

The boundary conditions discussed above are physical boundary conditions imposed by nature. Meanwhile in numerical modelling we should sometimes introduce additional conditions to properly define the mathematical problem under question.

In general, when the value of the variable is given at a boundary of the model domain, the condition is referred to as a Dirichlet boundary condition. When the gradient of the variable in a particular direction (usually normal to the boundary) is prescribed to the model boundary, the condition is called a Neumann boundary condition. Sometimes a linear combination of the two quantities is given, and in this case the boundary condition is referred to as a mixed boundary condition.

1.5 Analytical and numerical solutions

Mathematical models of geodynamic processes can be solved analytically or numerically. Analytical solutions are those that a researcher can obtain by solving mathematical models by using a pencil, a piece of paper, and his or her own brain activity. Simple mathematical models allow analytical solutions, which have been (and still are) of great importance because of their power: the solutions are precise and can be presented by exact formulas. However, the usefulness of this power is limited as many mathematical models of geodynamics are too complicated to be solved analytically.

Numerical solutions are those that researchers can obtain by solving numerical models using computational methods and computers. Numerical models allow the solution of complex problems of geodynamic processes, although the solutions are not exact. In some geodynamic applications an analytical solution to part of the complex problem can be implemented into the numerical model to make the model much more effective.

An analytical solution to a specified mathematical problem can be used to verify a numerical solution to the problem; in fact, it is the simplest way to benchmark a numerical code. Unfortunately, many two- and three-dimensional mathematical problems in geodynamics have no analytical solutions. But when analytical solutions to such problems are obtained in some cases, it is like finding water in a desert. For example, an analytical solution to a three-dimensional model of viscous flow (e.g. describing movements of salt diapirs in sedimentary basins) was recently obtained by Trushkov (2002). Considering the equations of slow viscous incompressible flow coupled with the equation for density advection, Trushkov (2002) found an exact solution to this set of partial differential equations. This solution can be used to verify numerical solutions to the problem of gravitational instability.

1.6 Rationale of numerical modelling

Only a few of the differential and partial differential equations describing geodynamical models can be solved exactly, and hence the equations are transformed into discrete equations to be solved numerically. Although the widespread access to high-performance computers has resulted in an over-reliance on numerical answers when there are other possibilities, and a corresponding false sense of security about the possibilities of serious numerical problems or errors, it is now possible without too much trouble to find solutions to most equations that are routinely encountered.

The rationale of the numerical modelling is described graphically in Fig. 1.1. The initial stage of numerical modelling is to describe geodynamic complex reality by a simplification of the reality; namely, to introduce the concept of the geodynamic problem, forces acting on the system (lithosphere, crust, mantle), physical parameters to be used in the modelling, etc.

A physical model is then developed to which the physical laws can be applied. The next step in the numerical modelling is to describe the physical model by means of mathematical equations. The comparison with observations allows the model to be tested (validated). If the mathematical model is found to be inadequate, it must be changed: the assumed process is not the correct one, or some significant factors have been missed. The mathematical model should be properly determined, at least after the numerical values of some still unknown parameters have been determined (that is, the model is tuned).

Once the mathematical model is developed, proper numerical tools and methods have to be determined, and relevant numerical codes (software) should be constructed (or otherwise obtained). The mathematical model should be transformed into the computational model containing discrete equations to be solved by using computers. An important element of numerical modelling is *verification* of the model, namely, the assessment of the accuracy

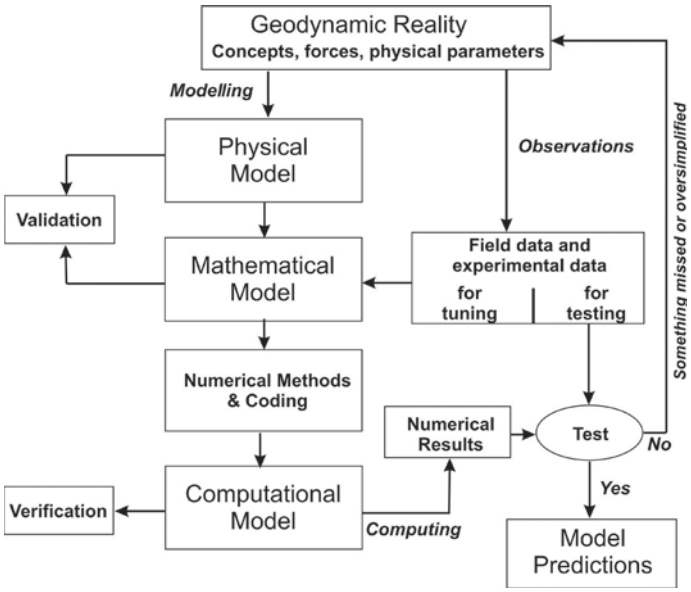

Fig. 1.1. Flowchart of numerical modelling.

of the solution to the computational model by comparison with known solutions (analytic or numerical). Once the computational model is verified, the model can be computed and numerical results obtained can be tested against observations. If there is good agreement between the numerical results and observed (field or experimental) data, the model results can be considered as the model predictions. Sometimes researchers dealing with numerical modelling make a serious mistake, when all available data have been used to tune the model and no data have been left to test its validity or, even worse, when the data used for the model tuning are employed to test model results.

1.7 Numerical methods: possibilities and limitations

By a numerical method we mean a procedure that permits us to obtain the solution to a mathematical problem with an arbitrary precision in a finite number of steps that can be performed rationally. The number of steps depends on the desired accuracy. A numerical method usually consists of a set of directions for the performance of certain arithmetical or logical operations in predetermined order. This set of directions must be complete and unambiguous. A set of directions to perform mathematical operations designed to lead to the solution of a given problem is called an *algorithm*.

Numerical methods came with the birth of electronic computers. Although many of the key ideas for numerical solution methods were established several centuries ago, they were of little use before computers appeared. Interest in numerical methods increased dramatically with the development of computer power. Computer solution of the equations

describing geodynamic processes has become so important that it occupies the attention of many researchers in geodynamics.

Numerical methods provide possibilities to obtain accurate solutions to geodynamic problems. However, the numerical results are always approximate. There are reasons for differences between computed results and observations. Errors arise from each part of the process used to produce numerical solution (we discuss sources of the errors in Section 1.9): (i) the physical model is too simplified compared with geodynamic reality; (ii) the equations (mathematical model) may contain approximations or idealisations; (iii) approximations are made in the discretisation process; and (iv) in solving the discrete equations, iterative methods are used and insufficient iterations are taken. Additionally, uncertainty in physical parameters can lead to differences between computed results and observations.

1.8 Components of numerical modelling

Numerical simulations in geodynamics enable one to analyse and to predict the dynamics of the Earth's interior. Computers are employed to solve numerically models of geodynamic processes. The basic elements of the numerical modelling are as follows: (i) a mathematical model describing geodynamics; (ii) a discretisation method to convert the mathematical equations into discrete equations to be solved numerically; (iii) numerical method(s) to solve the discretised equations; (iv) computer code(s) (i.e. software) to be developed or to be used, if already developed, that solve numerically the discrete equations; (v) computer hardware, which performs the calculations; (vi) results of numerical modelling to be visualised, analysed and interpreted by (vii) geoscientist(s).

Models of geodynamical processes described by partial differential (or integro-differential) equations cannot be solved analytically except in special cases. To obtain an approximate solution numerically, we have to use the discretisation method, which approximates the differential equations by a set of algebraic equations, which can then be solved on a computer. The approximations are applied to small domains in space and/or time so the numerical solution provides results at discrete locations in space and time. Much as the accuracy of observations depends on the quality of the tools used, the accuracy of numerical solutions depends on the quality of the discretisations used.

When the governing equations are known accurately, solutions of any desired accuracy can be achieved. However, for many geodynamic processes (e.g. thermo-chemical convection, mantle flow in the presence of phase transformations and complex rheology) the exact equations governing the processes are either not available or numerical solution of the full equations is not feasible. This requires the introduction of models. Even if we solve the equations exactly, the solution would not be a correct representation of reality. In order to validate the models, we have to rely on observations. Even when the exact treatment is possible, models are often needed to reduce the cost.

Discretisation errors can be reduced by using more accurate interpolation or approximations or by applying the approximations to smaller regions, but this usually increases the time and cost of obtaining the solution. Compromise is usually needed. We shall present some

schemes in detail but shall also point out ways of creating more accurate approximations. Compromises are also needed in solving the discretised equations. Direct solvers, which obtain accurate solutions, are seldom used in new codes, because they are too costly. Iterative methods are more common but the errors due to stopping the iteration process too soon need to be taken into account. The need to analyse and estimate numerical errors cannot be overemphasised.

Visualisation of numerical solutions using vectors, contours, other kinds of plots or movies (videos) is essential to interpret numerical results. However, there is the danger that an erroneous solution may look good but may not correspond to the true solution of a mathematical problem. It is especially important in the case of geodynamic problems because of the complex dynamics of the Earth components (crust, mantle and core). Sometimes incorrect numerical results are interpreted as physical phenomena. Users of commercial software should be especially careful, as the optimism of salesmen is legendary. Colour figures of results of numerical experiments sometimes make a great impression but are of no value if they are not quantitatively correct. Results must be examined critically before they are believed.

We follow Ferziger and Peric (2002) in the description of the components of numerical modelling.

Mathematical model. The starting point of numerical modelling is a mathematical model, i.e. the set of partial differential or integro-differential equations and boundary conditions. The equations governing a thermo-convective viscous flow in the Earth's mantle have been presented in Section 1.4. An appropriate model should be chosen for a geodynamic application (e.g. incompressible, viscous, two- or three-dimensional, etc.). As already mentioned, this model may include simplifications of the exact conservation laws. A solution method is usually designed for a particular set of equations.

Coordinate systems. The conservation equations can be written in many different forms, depending on the coordinate system. For example, one can select Cartesian, cylindrical, spherical and some others. The choice depends on the target problem, and may influence the discretisation method and grid type to be used.

Discretisation method. After selecting the mathematical model, one has to choose a suitable discretisation method, i.e. a method of approximating the differential equations by a set of algebraic equations for the variables at some set of discrete locations in space and time. There are many approaches, but the most popular at this time are finite difference, finite element and finite volume methods. Spectral methods were popular in the past, particularly for three-dimensional modelling, but their use is decreasing due to limitations. Other methods, like boundary element and discrete element methods are also used in geodynamic modelling, but less often.

Each type of method yields the same solution if the grid is very fine. However, some methods are more suitable to some classes of problems than others. The preference is often determined by the attitude of the developer. We shall discuss the pros and cons of the various methods later.

Numerical grid. This defines the discrete locations at which the unknowns are to be calculated. The grid is essentially a discrete representation of the geometric domain, on

which the problem is to be solved. It divides the solution domain into a finite number of sub-domains (e.g. elements, control volumes, points, etc.)

Structured (regular) grids consist of families of grid lines with the property that members of a single family do not cross each other and cross each member of the other families only once. The position of any grid point within the domain is uniquely identified by a set of two (in two-dimensional spaces) and three (in three-dimensional spaces) indices, e.g. (i, j, k). This is the simplest grid structure, since it is logically equivalent to a Cartesian grid. Each point has four nearest neighbours in two dimensions (2-D) and six in three dimensions (3-D). An example of a structured two-dimensional grid is illustrated in Fig. 1.2a. The simplest example of a numerical grid is an orthogonal grid.

For complex model domain geometries, *unstructured grids* are most appropriate. Such grids are best adapted to the finite element or finite volume approaches. The elements may have any shape, and there is no restriction on the number of neighbour elements or nodes. In practice, grids made of triangles or quadrilaterals in 2-D (see Fig. 1.2b), and tetrahedral or hexahedral in 3-D are most often used. Such grids can be generated automatically by existing algorithms (see Section 4.8).

Finite approximations. Following the choice of grid type, approximations should be selected to be used in the discretisation process. In a finite difference method, approximations for the derivatives at the grid points have to be selected. In the finite element method, one has to choose the shape functions (elements) and weight functions. The choice

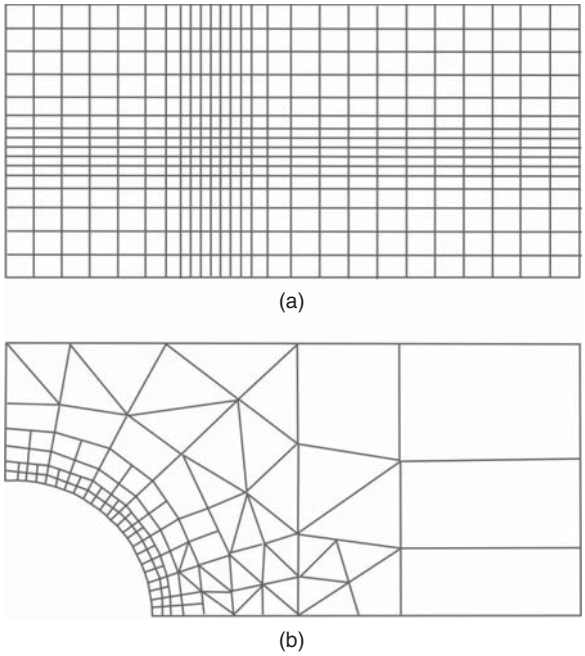

Fig. 1.2. **Examples of two-dimensional structured (a) and unstructured (b) grids.**

of the discretisation process influences the accuracy of the approximation. It also affects the difficulty of developing the solution method, coding it, debugging it, and the speed of the code. More accurate approximations involve more nodes and give fuller coefficient matrices. A compromise between simplicity, ease of implementation, accuracy and computational efficiency has to be made.

Solution method. Discretisation yields a large set of equations, and the method of solution depends on the problem. For non-stationary geodynamic processes, numerical methods for solving initial value problems for ordinary differential equations should be employed. At each time step a set of algebraic equations has to be solved. When the equations are non-linear, an iteration scheme is used to solve them. We present some solvers in Chapters 6 and 7.

Convergence criteria. When iterative methods are employed to solve discrete equations, convergence criteria should be established. Usually, there are two levels of iterations: *inner iterations*, within which the linear equations are solved, and *outer iterations*, that deal with the non-linearity and coupling of the equations. Deciding when to stop the iterative process on each level is important from the accuracy and efficiency points of view.

1.9 Properties of numerical methods

Numerical solution methods have certain important properties; they are summarised below following Ferziger and Peric (2002).

Consistency. The difference between the discretised and exact equations is called the *truncation error*. For a method to be consistent, the truncation error must become zero when the mesh spacing tends to zero. The truncation error is usually proportional to a power of the grid spacing Δx and/or the time step Δt. If the principal term of an equation is proportional to $(\Delta x)^n$ or $(\Delta t)^n$ we call the method an nth-order approximation; $n > 0$ is required for consistency. Even if the approximations are consistent, it does not necessarily mean that the solution of the set of discrete equations will become the exact solution to the differential equation in the limit of small step size. For this to happen, the solution method has to be *stable*.

Stability. A numerical solution method is stable if it does not magnify the errors that appear in the course of numerical solution process. For unsteady problems, stability guarantees that the method produces a bounded solution whenever the solution of the exact equation is bounded. For iterative methods, a stable method is one that does not diverge. Stability can be difficult to analyse, especially when solving non-linear and coupled equations with prescribed boundary conditions. There are few stability results for complicated discrete problems, so we should rely on experience and intuition. It is common to estimate the stability of a method for linear problems with constant coefficients without boundary conditions. The results obtained in this way can often be applied to more complex problems.

Convergence. A numerical method is said to be convergent if the solution of the discretised equations tends to the exact solution of the differential equation as the grid spacing tends to zero. For many non-linear problems in geodynamics, which are strongly influenced

by boundary conditions, the convergence (as well as *stability*) of a method is difficult to demonstrate. Therefore, convergence is usually checked using numerical experiments, i.e. repeating the calculation on a series of successively refined grids. If the method is stable and if all approximations used in the discretisation process are consistent, it is usually found that the solution converges to a grid-independent solution. For sufficiently small grid sizes, the rate of convergence is governed by the order of the principal truncation error component. This allows one to estimate the error in the solution.

Conservation. Since the equations to be solved are conservation laws, the numerical scheme should also respect these laws. This means that, at steady state and in the absence of sources, the amount of a conserved quantity leaving a closed volume is equal to the amount entering that volume. Conservation is an important property of the solution method, since it imposes a constraint on the solution error. If conservation of mass, momentum and energy are insured, the error can only improperly distribute these quantities over the solution domain. Non-conservative schemes can produce artificial sources, changing the balance both locally and globally. However, non-conservative schemes can be consistent and stable and therefore lead to correct solutions in the limit of very fine grids. The errors due to non-conservation are in most cases significant only on relatively coarse grids. Meanwhile it is difficult to estimate the size of the grid at which these errors are small enough, and hence conservative schemes are preferred.

Boundedness. Numerical solution should lie within proper *bounds*. Physically non-negative quantities (like density and viscosity) must always be positive. In the absence of sources, some equations (e.g. the heat equation for the temperature when no heat sources are present) require that the minimum and maximum values of the variable be found on the boundaries of the domain. These conditions should be inherited by the numerical approximation.

Accuracy. This is the most important property of numerical modelling. Numerical solutions of geodynamic problems are only *approximate solutions*. In addition to the errors that might be introduced in the course of the development of the solution algorithm, in programming or setting up the boundary conditions, numerical solutions always include three kinds of systematic error.

- *Modelling errors*, which are defined as the difference between the actual process and the exact solution of the mathematical model (modelling errors are introduced by simplifying the model equations, the geometry of the model domain, the boundary conditions, etc.).
- *Discretisation errors*, defined as the difference between the exact solution of the conservation equations and the exact solution of the algebraic system of equations obtained by discretising these equations.
- *Iteration errors*, defined as the difference between the iterative and exact solutions of the algebraic system of equations.

It is important to be aware of the existence of these errors, and even more to try to distinguish one from another. Various errors may cancel each other, so that sometimes a solution obtained on a coarse grid may agree better with the experiment than a solution on a finer grid – which, by definition, should be more accurate.

1.10 Concluding remarks

The success in numerical modelling of geodynamical processes is based on the following basic, but simple, rules.

(i) '*People need simplicity most, but they understand intricacies best*' (B. Pasternak, writer). Start from a simple mathematical model, which describes basic physical laws by a set of equations, and then develop to more complex models. Never start from a complex model, because in this case you cannot understand the contribution of each term of the equations to the solution of the model.

(ii) Use analytical methods at first (if possible) to solve the mathematical problem. If it is impossible to derive an analytical solution, transform the mathematical problem into a discrete problem.

(iii) Study the numerical methods behind your computer code. Otherwise it becomes difficult to distinguish true and erroneous solutions to the discrete problem, especially when your problem is complex enough.

(iv) Test your model against analytical and/or asymptotic solutions, and simple model examples. Develop benchmark analysis of different numerical codes and compare numerical results with laboratory experiments. Remember that the numerical tool you employ is not perfect, and there are small bugs in every computer code. Therefore the testing is the most important part of your numerical modelling.

(v) Learn relevant statements concerning the existence, uniqueness and stability of the solution to the mathematical and discrete problems. Otherwise you can solve an improperly posed problem, and the results of the modelling will be far from the true solution of your model problem.

(vi) Try to analyse numerical models of a geophysical phenomenon using as little as possible tuning of model parameters. Two tuning parameters already give enough possibility to constrain a model well with respect to observations. Data fitting is sometimes quite attractive and can take one far from the principal aim of numerical modelling in geodynamics: to understand geophysical phenomena and to simulate their dynamics. If the number of tuning model parameters are greater than two, test carefully the effect of each of the parameters on the modelled phenomenon. Remember: '*With four exponents I can fit an elephant*' (E. Fermi, physicist).

(vii) Make your numerical model as accurate as possible, but never put the aim to reach a great accuracy. '*Undue precision of computations is the first symptom of mathematical illiteracy*' (N. Krylov, mathematician).

How complex should a numerical model be? '*A model which images any detail of the reality is as useful as a map of scale 1:1*' (J. Robinson, economist). This message is quite important for geoscientists who study numerical models of complex geodynamical processes. Geoscientists will never create a model that represents the Earth dynamics in full complexity, but we should try to model the dynamics in such a way as to 'simulate' basic geophysical processes and phenomena.

Does a particular model have a predictive power? Each numerical model has a predictive power, otherwise the model is useless. The predictability of the model varies with its complexity. Remember that a solution to the numerical model is an approximate solution to the equations, which have been chosen in the belief that they describe dynamic processes of the Earth. Therefore, a numerical model predicts dynamics of the Earth as well as the mathematical equations describe this dynamics.

Computers and Structures 87 (2009) 802–811

Contents lists available at ScienceDirect

Computers and Structures

journal homepage: www.elsevier.com/locate/compstruc

Numerical techniques for solving the inverse retrospective problem of thermal evolution of the Earth interior

A. Ismail-Zadeh [a,b,c,*], A. Korotkii [d], G. Schubert [e], I. Tsepelev [d]

[a] Geophysikalishes Institut, Universität Karlsruhe, Hertzstrasse 16, Karlsruhe 76187, Germany
[b] MITPAN, Russian Academy of Sciences, Profsoyuznaya str. 84/32, Moscow 117997, Russia
[c] Institut de Physique du Globe de Paris, 4 Place Jussieu, Paris 75252, France
[d] Institute of Mathematics and Mechanics, Russian Academy of Sciences, S. Kovalevskoy ul. 16, Yekaterinburg 620219, Russia
[e] Department of Earth and Space Sciences and Institute of Geophysics and Planetary Physics, University of California, 3806 Geology Building, 595 Charles Young Drive East, Los Angeles, CA 90095-1567, USA

ARTICLE INFO

Article history:
Received 7 November 2008
Accepted 8 January 2009
Available online 23 February 2009

Keywords:
Data assimilation
Adjoint method
Quasi-reversibility method
Thermal mantle
structure

ABSTRACT

We consider an inverse (time-reverse) problem of thermal evolution of a viscous inhomogeneous incompressible heat-conducting fluid describing dynamics of the Earth's mantle. Present observations of geophysical fields (temperature, velocity) are incorporated in a three-dimensional dynamic model to determine the initial conditions of the fields. We present and compare numerical techniques for solving the inverse problem: backward advection, variational (adjoint), and quasi-reversibility methods. The methods are applied to restore the evolution of the mantle structures such as rising plumes and descending lithospheric plates.

1. Introduction

Many geodynamic problems can be described by mathematical models, i.e., by a set of partial differential equations and boundary and/or initial conditions defined in a specific domain. A mathematical model links the causal characteristics of a geodynamic process with its effects. The aim of the *direct* mathematical problem is to determine the relationship between the causes and effects of the geodynamic process and hence to find a solution to the mathematical problem for a given set of parameters and coefficients. An *inverse* problem is the opposite of a direct problem. An inverse problem is considered when there is a lack of information on the causal characteristics (but information on the effects of the geophysical process exists). Inverse problems can be subdivided into time-reverse or retrospective problems (e.g., to restore the development of a geodynamic process), coefficient problems (e.g., to determine the coefficients of the model equations and/or boundary conditions), geometrical problems (e.g., to determine the location of heat sources in a model domain or the geometry of the model boundary), and some others. In this paper, we will consider time-reverse (retrospective) problems of thermal evolution of the Earth's interior.

The Earth's mantle is heated from the Earth's core and from inside due to decay of radioactive elements. Since thermal convection in the mantle is described by heat advection and diffusion, one can ask: is it possible to tell, from the present temperature estimations of the Earth, something about the Earth's temperature in the geological past? Even though heat diffusion is irreversible in the physical sense, it is possible to predict accurately the heat transfer in the past without contradicting the basic thermodynamic laws.

The inverse retrospective problem of thermal convection in the mantle is an ill-posed problem, since the backward heat problem, describing both heat advection and conduction through the mantle backwards in time, possesses the properties of ill-posedness [1]. In particular, the solution to the problem does not depend continuously on the initial data. As for the existence and uniqueness of the solution to the backward heat problem, they are proven for several specific cases (we discuss it below). The authors do not know any proven statements about existence and uniqueness of the solution either to the direct or to the inverse thermal convection problem in three-dimensional cases.

To restore thermal structures in the mantle (e.g., *ascending plumes*, that is, hot mantle rocks rising through the surrounding colder rocks, and *descending lithospheric plates*, that is, cold and hence dense rocks subsiding into the hotter mantle) in the

* Corresponding author. Address: Geophysikalishes Institut, Universität Karlsruhe, Hertzstrasse 16, Karlsruhe 76187, Germany. Tel.: +49 721 6084610; fax: +49 721 71173.
E-mail addresses: Alik.Ismail-Zadeh@gpi.uka.de, aiz@ipgp.jussieu.fr (A. Ismail-Zadeh).

0045-7949/$ - see front matter © 2009 Elsevier Ltd. All rights reserved.
doi:10.1016/j.compstruc.2009.01.005

geological past, data assimilation techniques can be used to constrain the initial conditions for the mantle temperature and velocity from their present observations. The initial conditions so obtained can then be used to run forward models of mantle dynamics to restore the evolution of mantle structures. Data assimilation can be defined as the incorporation of observations (in the present) and initial conditions (in the past) in an explicit dynamic model to provide time continuity and coupling among the physical fields (e.g., velocity, temperature). The basic principle of data assimilation is to consider the initial condition as a control variable and to optimize the initial condition in order to minimize the discrepancy between the observations and the solution of the model.

If heat diffusion is neglected, the present mantle temperature and flow can be assimilated using the backward advection (BAD) into the past. Two- and three-dimensional numerical approaches to the solution of the inverse problem of the Rayleigh–Taylor instability were developed for a dynamic restoration of diapiric structures to their earlier stages (e.g. [2–5]). The mantle flow was modeled backwards in time from present-day mantle density heterogeneities inferred from seismic observations (e.g. [6,7]). Both direct (forward in time) and inverse (backward in time) problems of the heat (density) advection are well-posed. This is because the time-dependent advection equation has the same form of characteristics for the direct and inverse velocity field (the vector velocity reverses its direction, when time is reversed). Therefore, numerical algorithms used to solve the direct problem of the gravitational instability can also be used in studies of the time-reverse problems by replacing positive time-steps with negative ones.

In sequential filtering a numerical model is computed forward in time for the interval for which observations have been made, updating the model each time where observations are available. The sequential filtering was used to compute mantle circulation models [8,9]. Despite sequential data assimilation well adapted to mantle circulation studies, each individual observation influences the model state at later times. Information propagates from the geological past into the future, although our knowledge of the Earth's mantle at earlier times is much poor than that at present.

The variational (VAR) data assimilation method has been pioneered by meteorologists and used very successfully to improve operational weather forecasts (e.g. [10]). The data assimilation has also been widely used in oceanography (e.g. [11]) and in hydrological studies (e.g. [12]). However, the application of the method to problems of geodynamics (dynamics of the solid Earth) is still in its infancy. The use of VAR data assimilation in models of geodynamics (to estimate mantle temperature and flow in the geological past) has been put forward by Bunge et al. [13] and Ismail-Zadeh et al. [14,15] independently in 2003. The VAR approach by Ismail-Zadeh et al. [15] is computationally less expensive, because it does not involve the Stokes equation into the iterations between the direct and adjoint problems, and this approach admits the use of temperature-dependent viscosity. The VAR data assimilation algorithm was employed to restore numerically models of present prominent mantle plumes to their past stages [16] and to recover the structure of mantle plumes prominent in the past from that of present plumes weakened by thermal diffusion [17]. The VAR method was recently used to study dynamics models of thermal plumes and lithospheric plates in the mantle (e.g. [18,19]).

The use of the quasi-reversibility (QRV) method [20] implies the introduction into the backward heat equation of the additional term involving the product of a small regularization parameter and a higher order temperature derivative. The data assimilation in this case is based on a search of the best fit between the forecast model state and the observations by minimizing the regularization parameter. The modified QRV method was recently introduced in geodynamic modeling and employed to assimilate data in models of mantle dynamics [21,22].

The advances in numerical modeling and in data assimilation attract an interest of the geophysical community dealing with dynamics of the mantle structures. The aim of this paper is to review the VAR and QRV data assimilation methods introduced by the authors and to compare them with the BAD method used widely in geodynamic modeling for years.

2. Mathematical statement of the problem and numerical approach

We assume that the Earth's mantle behaves as a Newtonian incompressible fluid with a temperature-dependent viscosity and infinite Prandtl number [23]. The mantle flow is described by heat, motion, and continuity equations [23,24]. To simplify the governing equations, we make the Boussinesq approximation keeping the density constant everywhere except for buoyancy term in the equation of motion [25].

In the three-dimensional (3-D) model domain $\Omega = [0,x_1 = 3h] \times [0,x_2 = 3h] \times [0,x_3 = h]$, we consider the *boundary value problem for the flow velocity* (it includes the Stokes equation and the incompressibility equation subject to appropriate boundary conditions)

$$\nabla P = \mathrm{div}(\eta(T)\mathbf{E}) + RaT\mathbf{e}, \quad \mathbf{x} \in \Omega, \tag{1}$$

$$\mathrm{div}\,\mathbf{u} = 0, \quad \mathbf{x} \in \Omega, \tag{2}$$

$$\mathbf{u}\cdot\mathbf{n} = 0, \quad \partial\mathbf{u}_\tau/\partial\mathbf{n} = 0, \quad \mathbf{x} \in \partial\Omega, \tag{3}$$

and *the initial-boundary value problem for temperature* (it includes the heat equation subject to appropriate boundary and initial conditions)

$$\partial T/\partial t + \mathbf{u}\cdot\nabla T = \nabla^2 T + f, \quad t \in [0,\vartheta], \quad \mathbf{x} \in \Omega, \tag{4}$$

$$\sigma_1 T + \sigma_2 \partial T/\partial\mathbf{n} = T^*, \quad t \in [0,\vartheta], \quad \mathbf{x} \in \partial\Omega, \tag{5}$$

$$T(0,\mathbf{x}) = T_0(\mathbf{x}), \quad \mathbf{x} \in \Omega. \tag{6}$$

Here $\mathbf{x} = (x_1,x_2,x_3)$ are the Cartesian coordinates; T, t, $\mathbf{u}$, P, and η are dimensionless temperature, time, velocity, pressure, and viscosity, respectively; $\mathbf{E} = e_{ij}(\mathbf{u}) = \{\partial u_i/\partial x_j + \partial u_j/\partial x_i\}$ is the strain rate tensor; u_i are the velocity components; $\mathbf{e} = (0,0,1)$ is the unit vector; ∇ is the gradient operator; div is the divergence operator; f is the heat source; $\mathbf{n}$ is the outward unit normal vector at a point on the model boundary; $\mathbf{u}_\tau$ is the projection of the velocity vector onto the tangent plane at the same point on the model boundary; $[t = 0, t = \vartheta]$ is the model time interval; σ_1 and σ_2 are some piecewise smooth functions or constants such that $\sigma_1^2 + \sigma_2^2 \neq 0$.

The Rayleigh number is defined as $Ra = \alpha g \rho_{ref} \Delta T h^3 \eta_{ref}^{-1} \kappa^{-1}$, where α is the thermal expansivity, g is the acceleration due to gravity, ρ_{ref} and η_{ref} are the reference typical density and viscosity, respectively; ΔT is the temperature contrast between the lower and upper boundaries of the model domain; and κ is the thermal diffusivity. Length, temperature, and time are normalized by h, ΔT, and $h^2\kappa^{-1}$, respectively. The physical parameters of the fluid (temperature, velocity, pressure, viscosity, and density) are assumed to depend on time and on space coordinates. The mantle behaves as a Newtonian fluid on geological time scales, and a dimensionless temperature-dependent viscosity law [26] given by

$$\eta(T) = \exp\left(\frac{M}{T+G} - \frac{M}{0.5+G}\right)$$

is used in the modeling, where $M = [225/\ln(r)] - 0.25\ln(r)$, $G = 15/\ln(r) - 0.5$ and r is the viscosity ratio between the upper and lower boundaries of the model domain. We consider the impermeability condition with perfect slip on $\partial\Omega$. The perfect slip, no slip ($\mathbf{u} = 0$) or their combinations are used as boundary conditions in modeling of geodynamic processes [26]. In fact, our knowledge about the conditions of motion at boundaries of a geological domain is limited.

Meanwhile, the perfect slip (symmetry) condition approximates well conditions at boundaries of a geological domain in many practical case studies. When the rates of the Earth's surface motion are available, the data are used to constrain the conditions at the upper boundary of a numerical model.

Choosing σ_1, σ_2, and T_* in a proper way we can specify temperature or heat flux at the model boundaries. Surface temperatures and heat flux are known in many geological domains, and therefore the use of the data is straightforward in geodynamic modeling. By $\Gamma_u = \{\mathbf{x}:(\mathbf{x} \in \partial\Omega) \cap (x_3 = l_3)\}$, $\Gamma_l = \{\mathbf{x}:(\mathbf{x} \in \partial\Omega) \cap (x_3 = 0)\}$, and $\Gamma_v = \cup_{i=1,2}\{\mathbf{x} : (\mathbf{x} \in \Omega) \cap (x_i = 0)\} \cup \{\mathbf{x} : (\mathbf{x} \in \Omega) \cap (x_i = l_i)\}$, we denote the parts of the model boundary that $\Gamma_u \cup \Gamma_l \cup \Gamma_v = \partial\Omega$. We assume the constant temperature at the horizontal boundaries and zero heat flux at vertical boundaries of the model domain: $\sigma_1(t,\mathbf{x}) = 1$, $\sigma_2(t,\mathbf{x}) = 0$, and $T_*(t,\mathbf{x}) = 0$ at $(t,\mathbf{x}) \in [0,\vartheta] \times \Gamma_u$; $\sigma_1(t,\mathbf{x}) = 1$, $\sigma_2(t,\mathbf{x}) = 0$, and $T_*(t,\mathbf{x}) = 1$ at $(t,\mathbf{x}) \in [0,\vartheta] \times \Gamma_l$; and $\sigma_1(t,\mathbf{x}) = 0$, $\sigma_2(t,\mathbf{x}) = 1$, and $T_*(t,\mathbf{x}) = 0$ at $(t,\mathbf{x}) \in [0,\vartheta] \times \Gamma_v$.

The direct problem of thermo-convective flow is formulated as follows: find the velocity $\mathbf{u} = \mathbf{u}(t,\mathbf{x})$, the pressure $P = P(t,\mathbf{x})$, and the temperature $T = T(t,\mathbf{x})$ satisfying boundary value problem (1)–(3) and initial-boundary value problem (4)–(6). We can formulate the inverse problem in this case as follows: find the velocity, pressure, and temperature satisfying boundary value problem (1)–(3) and the final-boundary value problem which includes Eqs. (4) and (5) and the final condition:

$$T(\vartheta,\mathbf{x}) = T_\vartheta(\mathbf{x}), \quad \mathbf{x} \in \Omega, \tag{7}$$

where T_ϑ is the temperature at time $t = \vartheta$.

3. Variational (VAR) method for data assimilation

In this section, we describe a variational approach to 3-D numerical restoration of thermo-convective mantle flow (see details in [16]). The variational data assimilation is based on a search of the best fit between the forecast model state and the observations by minimizing an objective functional (a normalized residual between the target model and observed variables) over space at each time step. To minimize the objective functional over time, an assimilation time interval is defined and an adjoint model is typically used to find the derivatives of the objective functional with respect to the model states.

The method for variational data assimilation can be formulated with a weak constraint (a generalized inverse) where errors in the model formulation are taken into account [13] or with a strong constraint where the model is assumed to be perfect except for the errors associated with the initial conditions [15,16]. The generalized inverse of mantle convection considers model errors, data misfit and the misfit of parameters as control variables. Unfortunately the generalized inverse presents a tremendous computational challenge and is difficult to solve in practice, and therefore, the strong constraint makes the problem computationally tractable.

We consider the following objective functional:

$$J(\varphi) = \|T(\vartheta,\cdot;\varphi) - \chi(\cdot)\|^2, \tag{8}$$

where $\|\cdot\|$ denotes the norm in the space $L_2(\Omega)$ (the Hilbert space with the norm defined as $\|y\| = \left[\int_\Omega y^2(\mathbf{x})d\mathbf{x}\right]^{1/2}$). Since in what follows the dependence of solutions of the thermal boundary value problems on initial data is important, we introduce these data explicitly into the mathematical representation of temperature. Here $T(\vartheta,\cdot;\varphi)$ is the solution of the problem (4)–(6) at the final time ϑ, which corresponds to some (unknown as yet) initial temperature distribution $\varphi(\mathbf{x})$; $\chi(\mathbf{x}) = T(\vartheta,\mathbf{x};T_0)$ is the known temperature distribution at the final time, which corresponds to the initial temperature $T_0(\cdot)$. The functional has its unique global minimum at value $\varphi \equiv T_0$ and $J(T_0) \equiv 0$, $\nabla J(T_0) \equiv 0$. The uniqueness of the global minimum of the objective functional follows from the uniqueness of the solution of the relevant boundary value problem for the heat equation and from a strong convexity of the functional [29]. Therefore, if a solution to the backward heat problem exists, the solution is unique.

To find the minimum of the functional we employ the gradient method ($k = 0,\ldots,k_*,\ldots$):

$$\varphi_{k+1} = \varphi_k - \beta_k \nabla J(\varphi_k), \quad \varphi_0 = \widetilde{T}, \tag{9}$$

$$\beta_k = \begin{cases} J(\varphi_k)/\|\nabla J(\varphi_k)\|, & 0 \leqslant k \leqslant k_*, \\ 1/(k+1), & k > k_*, \end{cases} \tag{10}$$

where $\widetilde{T}$ is an initial temperature guess, and k_* is a natural number. The minimization method belongs to a class of limited-memory quasi-Newton methods [27], where approximations to the inverse Hessian matrices are chosen to be the identity matrix. The gradient of the objective functional $\nabla J(\varphi_k)$ decreases steadily with the number of iterations providing the convergence, although the absolute value of $J(\varphi_k)/\|\nabla J(\varphi_k)\|$ increases with the number of iterations, and it can result in instability of the iteration process. To enhance the rate of convergence and to stabilize the solution at the same time, we perform initially several iterations ($k_* = 5$) using $\beta_k = J(\varphi_k)/\|\nabla J(\varphi_k)\|$ and then replace the expression by $\beta_k = 1/(k+1)$ as described in (10).

Let us assume that the gradient of the objective functional $\nabla J(\varphi_k)$ is computed with an error and $\|\nabla J_\delta(\varphi_k) - \nabla J(\varphi_k)\| < \delta$, where $\nabla J_\delta(\varphi_k)$ is the computed value of the gradient and δ is a constant. We introduce the function $\varphi^\infty = \varphi_0 - \sum_{k=1}^\infty \beta_k \nabla J(\varphi_k)$, assuming that the infinite sum exists, and the function $\varphi_\delta^\infty = \varphi_0 - \sum_{k=1}^\infty \beta_k \nabla J_\delta(\varphi_k)$ as the computed value of φ^∞. For stability of the iteration method (9), the following inequality should be met:

$$\|\varphi_\delta^\infty - \varphi^\infty\| = \left\|\sum_{k=1}^\infty \beta_k(\nabla J_\delta(\varphi_k) - \nabla J(\varphi_k))\right\| \leqslant \sum_{k=1}^\infty \beta_k \|\nabla J_\delta(\varphi_k) - \nabla J(\varphi_k)\| \leqslant \delta \sum_{k=1}^\infty \beta_k.$$

If $\beta_k = 1/k^p$ and $p > 1$, the sum $\sum_{k=1}^\infty \beta_k$ is finite. We use $p = 1$, but the number of iterations is limited, and therefore the iteration method is conditionally stable, although the convergence rate of these iterations is low.

The minimization algorithm requires the calculation of the gradient of the objective functional, ∇J. This can be done through the use of the *adjoint* problem for the problem (4)–(6) with the relevant boundary and initial conditions. In the case of the heat problem, the adjoint problem can be represented in the following form:

$$\partial\Psi/\partial t + \mathbf{u} \cdot \nabla\Psi + \nabla^2\Psi = 0, \quad \mathbf{x} \in \Omega,\ t \in (0,\vartheta), \tag{11}$$

$$\sigma_1\Psi + \sigma_2 \partial\Psi/\partial\mathbf{n} = 0, \quad \mathbf{x} \in \partial\Omega,\ t \in (0,\vartheta), \tag{12}$$

$$\Psi(\vartheta,\mathbf{x}) = 2(T(\vartheta,\mathbf{x};\varphi) - \chi(\mathbf{x})), \quad \mathbf{x} \in \Omega. \tag{13}$$

We showed that the solution to the adjoint problem (11)–(13) is the gradient of the objective functional (8): $\Psi(0,\cdot) = \nabla J(\varphi)$ [15].

Implementation of minimization algorithms requires the evaluation of both the objective functional (8) and its gradient ∇J. Each evaluation of the objective functional requires an integration of the model problem (4)–(6), whereas the gradient is obtained through the backward integration of the adjoint problem (11)–(13). The performance analysis shows that the CPU time required to evaluate the gradient J is about the CPU time required to evaluate the objective functional itself, and this is because the direct and adjoint heat problems are described by the same equations. Information on the properties of the Hessian matrix ($\nabla^2 J$) is important in many aspects of minimization problems [28]. To obtain sufficient conditions for the existence of the minimum of the problem, the Hessian matrix must be positive definite at T_0 (optimal initial

temperature). However, an explicit evaluation of the Hessian matrix in our case is prohibitive due to the number of variables.

We describe now the algorithm for numerical solution of the inverse problem (1)–(6) of thermal convection in the mantle using the VAR method. A uniform partition of the time axis is defined at points $t_n = \vartheta - \delta t n$, where δt is the time step, and n successively takes integer values from 0 to some natural number $m = \vartheta/\delta t$. At each subinterval of time $[t_{n+1}, t_n]$, the search of the temperature T and flow velocity $\mathbf{u}$ at $t = t_{n+1}$ consists of the following basic steps:

Step 1. Given the temperature $T = T(t_n,\mathbf{x})$ at $t = t_n$ we solve a set of linear algebraic equations derived from (1)–(3) in order to determine the velocity $\mathbf{u}$.
Step 2. The 'advective' temperature $T_{adv} = T_{adv}(t_{n+1},\mathbf{x})$ is determined by solving the advection heat equation backward in time, neglecting the diffusion term in (4). This can be done by replacing positive time-steps by negative ones. Given the temperature $T = T_{adv}$ at $t = t_{n+1}$ Steps 1 and 2 are then repeated to find the velocity $\mathbf{u}_{adv} = \mathbf{u}(t_{n+1},\mathbf{x};T_{adv})$.
Step 3. The heat equation (4) is solved with the boundary condition (5) and the initial condition $\varphi_k(\mathbf{x}) = T_{adv}(t_{n+1},\mathbf{x})$, $k = 0,1,2,\ldots,m$ forward in time using velocity $\mathbf{u}_{adv}$ in order to find $T(t_n,\mathbf{x};\varphi_k)$.
Step 4. The adjoint equation of (11) is then solved backward in time with the boundary condition (12) and the initial condition $\Psi(t_n,\mathbf{x}) = 2(T(t_n,\mathbf{x};\varphi_k) - \chi(\mathbf{x}))$ using velocity $\mathbf{u}$ in order to determine $\nabla J(\varphi_k) = \Psi(t_{n+1},\mathbf{x};\varphi_k)$.
Step 5. The coefficient β_k is determined from (10), and the temperature is updated (i.e. φ_{k+1} is determined) from (9).
Steps 3–5 are repeated until

$$\delta\varphi_n = J(\varphi_n) + \|\nabla J(\varphi_n)\|^2 < \varepsilon, \tag{14}$$

where ε is a small constant. Temperature φ_k is then considered to be the approximation to the target value of the initial temperature $T(t_{n+1},\mathbf{x})$. And finally, Step 1 is used to determine the flow velocity $\mathbf{u}(t_{n+1},\mathbf{x};T(t_{n+1},\mathbf{x}))$. Step 2 introduces a pre-conditioner to accelerate the convergence of temperature iterations in Steps 3–5 at high Rayleigh number. At low *Ra*, Step 2 is omitted and $\mathbf{u}_{adv}$ is replaced by $\mathbf{u}$. After these algorithmic steps, we obtain temperature $T = T(t_n,\mathbf{x})$ and flow velocity $\mathbf{u} = \mathbf{u}(t_n,\mathbf{x})$ corresponding to $t = t_n$, $n = 0,\ldots,m$. Based on the obtained results, we can use interpolation to reconstruct, when required, the entire process on the time interval $[0,\vartheta]$ in more detail.

Thus, at each subinterval of time we apply the VAR method to the heat equation only, iterate the direct and conjugate problems for the heat equation in order to find temperature, and determine backward flow from the Stokes and continuity equations twice (for 'advective' and 'true' temperatures). The solution of the backward heat problem is therefore reduced to solutions of series of forward problems, which are known to be well-posed [29].

Although the VAR data assimilation technique described above can theoretically be applied to many problems of mantle and lithosphere dynamics, a practical implementation of the technique for modeling of real geodynamic processes backward in time (to restore the temperature and flow pattern in the past) is not a simple task. Smoothness of the input (present) temperature and of the target (initial) temperature in the past is an important factor in backward modeling.

Samarskii et al. [30] studied a one-dimensional (1-D) backward heat diffusion problem and showed that the solution to this problem becomes noisy if the initial temperature guess is slightly perturbed, and the amplitude of this noise increases with the initial perturbations of the temperature guess. They suggested using a special filter to reduce the noise and illustrate the efficiency of the filter. This filter is based on the replacement of iterations (9) by the following iterative scheme:

$$\mathbf{B}(\varphi_{k+1} - \varphi_k) = -\beta_k \nabla J(\varphi_k), \tag{15}$$

where $\mathbf{B}y = y - \nabla^2 y$. Unfortunately, employment of this filter increases the number of iterations to obtain the target temperature and it becomes quite expensive computationally, especially when the model is three-dimensional. In practice, our approach to this problem was to run the model backward to the point of time when the noise becomes relatively large. Another way to reduce the noise is to employ high-order adjoint [31] or regularization (e.g. [20,32]) techniques.

4. Quasi-reversibility (QRV) method for data assimilation

In this section, we describe a quasi-reversibility approach to 3-D numerical restoration of thermo-convective mantle flow (see details in [21]). The principal idea of the quasi-reversibility method is based on the transformation of an ill-posed problem into a well-posed problem [20]. In the case of the backward heat equation, this implies an introduction of an additional term into the equation, which involves the product of a small regularization parameter and higher order temperature derivative. The additional term should be sufficiently small compared to other terms of the heat equation and allow for simple additional boundary conditions. The data assimilation in this case is based on a search of the best fit between the forecast model state and the observations by minimizing the regularization parameter. The regularized backward heat problem has the unique solution [20,36,40].

The transformation to the regularized backward heat problem is not only a mathematical approach to solving ill-posed backward heat problems, but has some physical meaning: it can be explained on the basis of the concept of relaxing heat flux for heat conduction (e.g. [33]). The classical Fourier heat conduction theory provides the infinite velocity of heat propagation in a region. The instantaneous heat propagation is unrealistic, because the heat is a result of the vibration of atoms and the vibration propagates in a finite speed [34]. To accommodate the finite velocity of heat propagation, a modified heat flux model was proposed by Vernotte [33] and Cattaneo [35].

To solve the inverse problem by the QRV method we suggested to consider the following regularized backward heat problem to define temperature in the past from the known temperature $T_\vartheta(\mathbf{x})$ at present time $t = \vartheta$ [21]:

$$\partial T_\beta/\partial t - \mathbf{u}_\beta \cdot \nabla T_\beta = \nabla^2 T_\beta + f - \beta \Lambda(\partial T_\beta/\partial t), \quad t \in [0,\vartheta],\ \mathbf{x} \in \Omega, \tag{16}$$

$$\sigma_1 T_\beta + \sigma_2 \partial T_\beta/\partial \mathbf{n} = T_*, \quad t \in (0,\vartheta),\ \mathbf{x} \in \partial\Omega, \tag{17}$$

$$\sigma_1 \partial^2 T_\beta/\partial \mathbf{n}^2 + \sigma_2 \partial^3 T_\beta/\partial \mathbf{n}^3 = 0, \quad t \in (0,\vartheta),\ \mathbf{x} \in \partial\Omega, \tag{18}$$

$$T_\beta(\vartheta,\mathbf{x}) = T_\vartheta(\mathbf{x}), \quad \mathbf{x} \in \Omega, \tag{19}$$

where $\Lambda(T) = \partial^4 T/\partial x_1^4 + \partial^4 T/\partial x_2^4 + \partial^4 T/\partial x_3^4$, and the boundary value problem to determine the fluid flow:

$$\nabla P_\beta = -\mathrm{div}[\eta(T_\beta)\mathbf{E}(\mathbf{u}_\beta)] + RaT_\beta \mathbf{e}, \quad \mathbf{x} \in \Omega, \tag{20}$$

$$\mathrm{div}\,\mathbf{u}_\beta = 0, \quad \mathbf{x} \in \Omega, \tag{21}$$

$$\mathbf{u}_\beta \cdot \mathbf{n} = 0,\ \partial(\mathbf{u}_\beta)_\tau/\partial \mathbf{n} = 0, \quad \mathbf{x} \in \partial\Omega. \tag{22}$$

Hereinafter we refer to temperature T_ϑ as the input temperature for the problem (16)–(22). The core of the transformation of the heat equation is the addition of a high-order differential expression $\Lambda(\partial T_\beta/\partial t)$ multiplied by a small parameter $\beta > 0$. Note that Eq. (18) is added to the boundary conditions to properly define the regularized backward heat problem. The solution to the regularized backward heat problem is stable for $\beta > 0$, and the approximate solution to (16)–(22) converges to the solution of (1)–(5) and (7) in some

spaces, where the conditions of well-posedness are met [36]. Thus, the inverse problem of thermo-convective mantle flow is reduced to determination of the velocity $\mathbf{u}_\beta = \mathbf{u}_\beta(t,\mathbf{x})$, the pressure $P_\beta = P_\beta(t,\mathbf{x})$, and the temperature $T_\beta = T_\beta(t,\mathbf{x})$ satisfying (16)–(22).

We seek a maximum of the following functional with respect to the regularization parameter β:

$$\delta - \|T(t=\vartheta,\cdot;T_{\beta_k}(t=0,\cdot)) - \chi(\cdot)\| \to \max_k, \tag{23}$$

$$\beta_k = \beta_0 q^{k-1}, \quad k = 1,2,\ldots,\Re, \tag{24}$$

where $T_k = T_{\beta_k}(t=0,\cdot)$ is the solution to the regularized backward heat problem (16)–(18) at $t=0$; $T(t=\vartheta,\cdot;T_k)$ is the solution to the heat problem (4) and (5) at the initial condition $T(t=0,\cdot) = T_k$ at time $t=\vartheta$; χ is the known temperature at $t=\vartheta$ (the input data on the present temperature); small parameters $\beta_0 > 0$ and $0 < q < 1$ are defined below; and $\delta > 0$ is a given accuracy. When q tends to unity, the computational cost becomes large; and when q tends to zero, the optimal solution can be missed.

The prescribed accuracy δ is composed from the accuracy of the initial data and the accuracy of computations. When the input noise decreases and the accuracy of computations increases, the regularization parameter is expected to decrease. However, estimates of the initial data errors are usually inaccurate. Estimates of the computation accuracy are not always known, and when they are available, the estimates are coarse. In practical computations, it is more convenient to minimize the following functional with respect to (24)

$$\|T_{\beta_{k+1}}(t=0,\cdot) - T_{\beta_k}(t=0,\cdot)\| \to \min_k, \tag{25}$$

where misfit between temperatures obtained at two adjacent iterations must be compared. To implement the minimization of temperature residual (23), the inverse problem (16)–(22) must be solved on the entire time interval as well as the direct problem (1)–(6) on the same time interval. This at least doubles the amount of computations. The minimization of functional (25) has a lower computational cost, but it does not rely on a priori information.

We describe now the numerical algorithm for solving the inverse problem of thermal convection in the mantle using the QRV method. Consider a uniform temporal partition $t_n = \vartheta - \delta t n$ (as defined in Section 3) and prescribe some values to parameters β_0, q, and $\Re$ (e.g., $\beta_0 = 10^{-3}$, $q = 0.1$, and $\Re = 10$). A sequence of the values of the regularization parameter $\{\beta_k\}$ is defined according to (24). For each value $\beta = \beta_k$ model temperature and velocity are determined in the following way.

Step 1. Given the temperature $T_\beta = T_\beta(t,\cdot)$ at $t = t_n$, the velocity $\mathbf{u}_\beta = \mathbf{u}_\beta(t_n,\cdot)$ is found by solving problem (20)–(22). This velocity is assumed to be constant on the time interval $[t_{n+1}, t_n]$.

Step 2. Given the velocity $\mathbf{u}_\beta = \mathbf{u}_\beta(t_n,\cdot)$, the new temperature $T_\beta = T_\beta(t,\cdot)$ at $t = t_{n+1}$ is found on the time interval $[t_{n+1}, t_n]$ subject to the final condition $T_\beta = T_\beta(t_n,\cdot)$ by solving problem (16)–(19).

Step 3. Upon the completion of Steps 1 and 2 for all $n = 0,1,\ldots,m$, the temperature $T_\beta = T_\beta(t_n,\cdot)$ and the velocity $\mathbf{u}_\beta = \mathbf{u}_\beta(t_n,\cdot)$ are obtained at each $t = t_n$. Based on the computed solution we can find the temperature and flow velocity at each point of time interval $[0,\vartheta]$ using interpolation.

Step 4a. The direct problem (4)–(6) is solved assuming that the initial temperature is given as $T_\beta = T_\beta(t=0,\cdot)$, and the temperature residual (23) is found. If the residual does not exceed the predefined accuracy, the calculations are terminated, and the results obtained at Step 3 are considered as the final ones. Otherwise, parameters β_0, q, and $\Re$ entering Eq. (24) are modified, and the calculations are continued from Step 1 for new set $\{\beta_k\}$.

Step 4b. The functional (25) is calculated. If the residual between the solutions obtained for two adjacent regularization parameters satisfies a predefined criterion (the criterion should be defined by a user, because no a priori data are used at this step), the calculation is terminated, and the results obtained at Step 3 are considered as the final ones. Otherwise, parameters β_0, q, and $\Re$ entering Eq. (24) are modified, and the calculations are continued from Step 1 for new set $\{\beta_k\}$.

In a particular implementation, either Step 4a or Step 4b is used to terminate the computation. This algorithm allows (i) organizing a certain number of independent computational modules for various values of the regularized parameter β_k that find the solution to the regularized problem using Steps 1–3 and (ii) determining *a posteriori* an acceptable result according to Step 4a or Step 4b.

Stability of the solution to (16)–(19) is difficult to analyse. Samarskii and Vabischevich [36] estimated the stability of the solution to 1-D regularized backward heat problem with respect to the initial condition expressed in the form $T_\beta(t=t^*,x) = T^*_\beta$:

$$\|T_\beta(t,x)\| + \beta\|\partial T_\beta(t,x)/\partial x\| \leqslant C(\|T^*_\beta\| + \beta\|\partial T^*_\beta/\partial x\|)\exp[(t^*-t)\beta^{-1/2}],$$

where C is a constant. According to this estimation, the natural logarithm of errors will increase in a direct proportion to time and inversely to the root square of the regularization parameter.

5. Numerical methods

To solve the heat problem (4)–(6) and the regularized heat problem (16)–(19), finite differences are used to derive discrete equations. We employ (i) the characteristic-based semi-Lagrangian (CBSL) method [37,38] to calculate the derivatives of the convective term in the heat equation (4); (ii) the total variation diminishing (TVD) method [39] to calculate the derivatives of the convective term in the regularized heat equation (16); (iii) central differences to approximate the derivatives of the diffusion and regularizing terms in (4) and (16), respectively; and (iv) the two-layered additively averaged scheme to represent the 3-D spatial discrete operators associated with the diffusion and regularizing terms as 1-D discrete operators, and the component-wise splitting method to solve the set of the discrete equations [40].

The Eulerian finite-element method is employed to solve the Stokes problems (1)–(3) and (20)–(22). The numerical approach is based on the representation of the flow velocity by a two-component vector potential [41] eliminating the incompressibility equation from the relevant boundary value problems. This potential is approximated by tri-cubic splines, which allows one to efficiently interpolate the velocity field. Such a procedure results in a set of linear algebraic equations with a symmetric positive-definite banded matrix. We solve the set of discrete equations by the conjugate gradient method [42]. A detailed description of the numerical methods used in the modelling is presented in appendices of [21].

To stabilize the numerical solution to time-dependent advection-dominated problems, several techniques were introduced (e.g. [43,44]). When oscillations arise, the numerical solution will have larger total variation of temperature (that is, the sum of the variations of temperature over the whole computational domain will increase with oscillations). The TVD method (we employ in the modelling) is designed to yield well-resolved, non-oscillatory discontinuities by enforcing that the numerical schemes generate solutions with non-increasing total variations of temperature in time, thus no spurious numerical oscillations are generated [45]. The TVD method describes convection problems with large temperature gradients very well, because it is at most first-order accurate at local temperature extrema [46].

Accuracy of the numerical solution to the 3-D Stokes equation coupled with the advection equation was checked by comparing the solution with the partial analytical solution to the problem [47]. Because the 3-D spatial discrete operator associated with the diffusion term of the heat equation was split into 1-D discrete operators, Korotkii and Tsepelev [48] tested the stability of the solver in a 1-D case. Accuracy of the numerical solutions to the Stokes and heat problems was tested by the following procedure: (i) employ a trial continuously differentiable function and insert it instead of the unknown function; (ii) obtain the right-hand side of the governing equation and solve numerically the equation with the right-hand side so obtained; and (iii) finally compare the numerical solution with the trial function [41].

6. Applications of data assimilation methods

6.1. Restoration of mantle plumes: synthetic case study

Thermal plumes in the Earth's mantle evolve in three distinguishing stages: (i) immature, i.e., an origin and initial rise of the plumes; (ii) mature, i.e., plume–lithosphere interaction, gravity spreading of plume head and development of overhangs beneath the bottom of the lithosphere, and partial melting of the plume material; and (iii) overmature, i.e., slowing-down of the plume rise and fading of the mantle plumes due to thermal diffusion [17]. The ascent and evolution of mantle plumes depend on the properties of the source region (that is, the thermal boundary layer) and the viscosity and thermal diffusivity of the ambient mantle. The properties of the source region determine temperature and viscosity of the mantle plumes. Structure, flow rate, and heat flux of the plumes are controlled by the properties of the mantle through which the plumes rise. While properties of the lower mantle (e.g., viscosity, thermal conductivity) are relatively constant during about 150 million years lifetime of most plumes [23], source region properties can vary substantially with time as the thermal basal boundary layer feeding the plume is depleted of hot material. Complete local depletion of this boundary layer cuts the plume off from its source. Laboratory [49] and numerical experiments forward in time [17] show that thermal plumes start disappearing from bottom up due to a week feeding of plumes by the hot material from the boundary layer.

To compare how three techniques for data assimilation can restore the prominent state of the thermal plumes in the past from their 'present' weak state, we develop initially a forward model from the prominent state of the plumes (Fig. 1a) to their diffusive state in 100 million years (Fig. 1b). To do it we solve numerically Eqs. (1)–(6) in the domain Ω (where $h = 2800$ km), which is divided into $50 \times 50 \times 50$ rectangular finite elements to approximate the vector velocity potential by tri-cubic splines; a uniform grid $148 \times 148 \times 148$ is employed for approximation of temperature, velocity, and viscosity.

We apply the QRV, VAR, and BAD methods to restore the plumes from their weak state and present the results of the restoration and temperature residuals (between the initial temperature for the forward model and the temperature assimilated to the same age) in Fig. 1. The VAR method (Fig. 1d and g) provides the best performance for the diffused plume restoration. The BAD method (Fig. 1e and h) cannot restore the diffused parts of the plumes, because temperature is only advected backward in time. The QRV method (Fig. 1c and f) restores the diffused thermal plumes, meanwhile the restoration results are not so perfect as in the case of VAR method. Although the accuracy of the QRV data assimilation is lower compared to the VAR data assimilation, the QRV method does not require any additional smoothing of the input data and filtering of temperature noise as the VAR method does.

The iteration scheme (9) and (10) of the VAR method provides the solution of high accuracy because of the following reasons. The function $\chi(\cdot)$ is not an arbitrary function, but it is the solution to (4)–(6). The adjoint problem (11)–(13) is solved by the same numerical method and the same numerical code as the direct problem (4)–(6). To improve the solution accuracy (as well as the solution convergence), we introduce preconditioned velocity $\mathbf{u}_{adv}$ reducing errors associated with an inaccuracy in determination of $\chi(\cdot)$.

6.2. Restoration of a descending lithosphere: geophysical case study

In this section, we present a quantitative model of the thermal evolution of the descending lithospheric slab in the SE-Carpathians using the QRV method for assimilation of present crust/mantle temperature and flow in the geological past [22]. The model of the present temperature of the crust and upper mantle is estimated from body wave seismic velocity anomalies [50] and heat flux data [51] and is assimilated into Miocene times (22 million years ago).

To minimize boundary effects, the studied region (650×650 km^2 and 440 km deep, see Fig. 2a) has been bordered horizontally by 200 km area and extended vertically to the depth of 670 km. Therefore we consider a rectangular 3-D domain $\Omega = [0, x_1 = l_1 = 1050\ \text{km}] \times [0, x_2 = l_2 = 1050\ \text{km}] \times [0, x_3 = h = 670\ \text{km}]$ for assimilation of present temperature and mantle flow beneath the SE-Carpathians.

Our ability to reverse mantle flow is limited by our knowledge of past movements in the region, which are well constrained only in some cases. In reality, the Earth's crust and lithospheric mantle are driven by mantle convection and the gravitational pull of dense descending slabs. However, when a numerical model is constructed for a particular region, external lateral forces can influence the regional crustal and uppermost mantle movements. Yet in order to make useful predictions that can be tested geologically, a time-dependent numerical model should include the history of surface motions. Since this is not currently achievable in a dynamical way, we prescribe surface motions using velocity boundary conditions.

The heat flux through the vertical boundaries of the model domain Ω is set to zero. The upper and lower boundaries are assumed to be isothermal surfaces. The present temperature above 440 km depth is derived from the seismic velocity anomalies and heat flow data. We use the adiabatic geotherm for potential temperature 1750 K [52] to define the present temperature below 440 km (where seismic tomography data are not available). Eqs. (16)–(22) with the specified boundary and initial conditions are solved numerically.

The numerical models, with a spatial resolution of 7 km × 7 km × 5 km, were run on parallel computers. To estimate the accuracy of the results of data assimilation, we employ the temperature and mantle flow restored to the time of 22 million years ago as the initial condition for a model of the slab evolution forward in time, run the model to the present, and analyze the temperature residual (the difference between the present temperature and that predicted by the forward model with the restored temperature as an initial temperature distribution). The maximum temperature residual does not exceed 50°.

A sensitivity analysis was performed to understand how stable is the numerical solution to small perturbations of input (present) temperatures. The model of the present temperature has been perturbed randomly by 0.5–2% and then assimilated to the past to find the initial temperature. A misfit between the initial temperatures related to the perturbed and unperturbed present temperature is rather small (2–4%) which proves that the solution is stable.

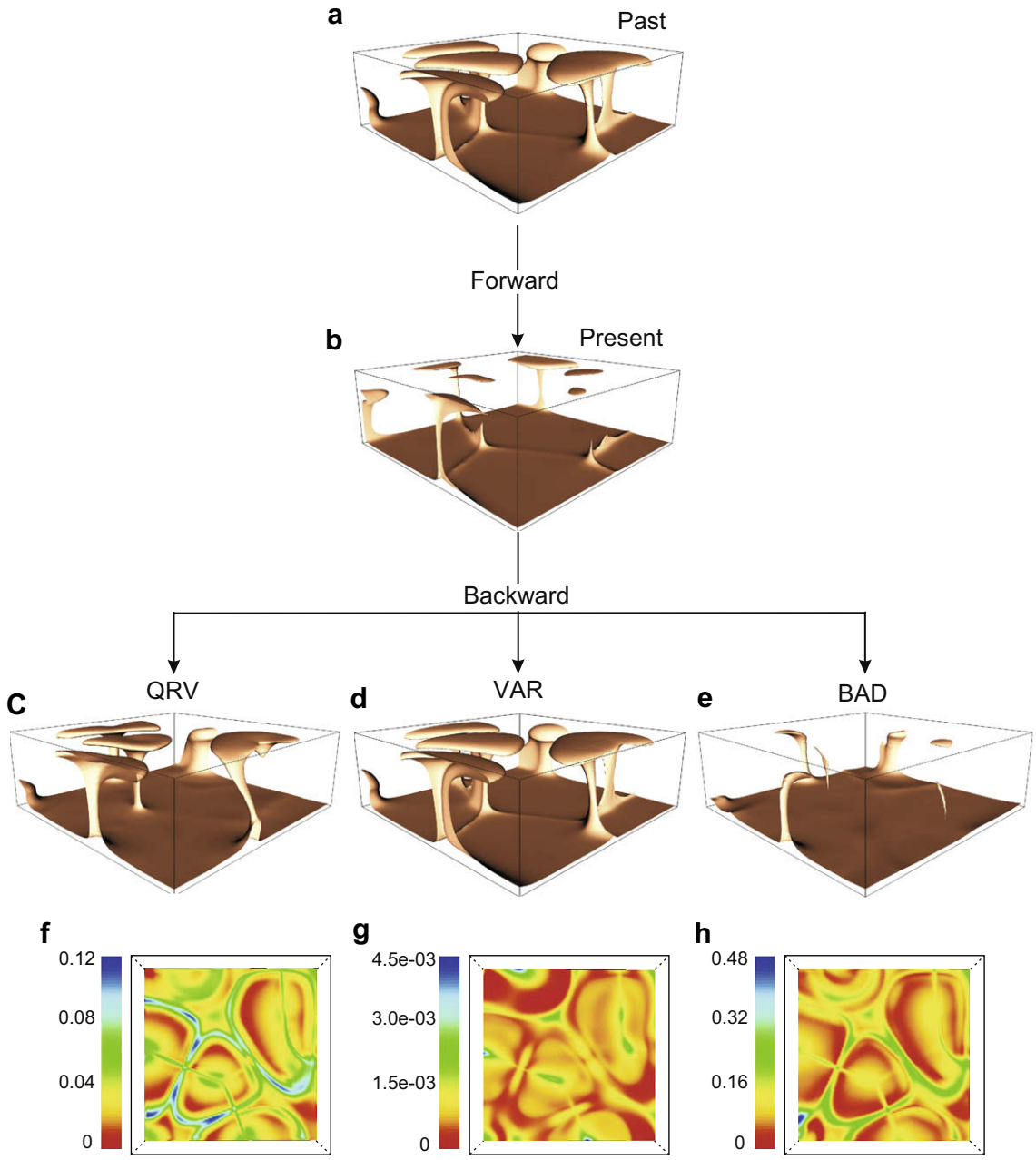

Fig. 1. Model of mantle plume evolution forward in time (a and b; $r = 20$). Assimilation of the mantle temperature and flow to the time of 100 million years ago and temperature residuals between the temperature model in the past (a) and the temperature assimilated to the same age starting from the present temperature model (b), using the QRV (c and f; $\beta = 10^{-7}$), VAR (d and g), and BAD (e and h) methods, respectively.

Fig. 2a presents the 3-D thermal image of the slab and pattern of contemporary flow induced by the descending slab. Note that the direction of the flow is reversed, because we solve the problem backward in time: cold slab move upward during the numerical modeling. The 3-D flow is rather complicated: toroidal (in horizontal planes) flow at depths between about 100 and 200 km coexists with poloidal (in vertical planes) flow. The geometry of the restored slab is shown in Fig. 2b–d. The numerical results were compared to that obtained by the backward advection of temperature (using the BAD method): the maximum temperature residual in the case of the BAD assimilation is found to be about 360°. The neglect of heat diffusion leads to an inaccurate restoration of mantle temperature, especially in the areas of low temperature and high viscosity. The similar results for the BAD data assimilation have been obtained in the synthetic case study (see Fig. 1e and h). The VAR method was not employed to assimilate the present temperature, because computations in this case become quite time-consuming due to the unavoidable need to smooth the solution and to filter temperature noise.

7. Comparison of the methods for data assimilation

In this section, we compare the VAR, QRV, and BAD methods in terms of solution stability, convergence, and accuracy, time interval for data assimilation, analytical and algorithmic works, and computer performance (see Tables 1 and 2). The VAR data assimilation assumes that the direct and adjoint problems are constructed and solved iteratively forward in time. The structure of

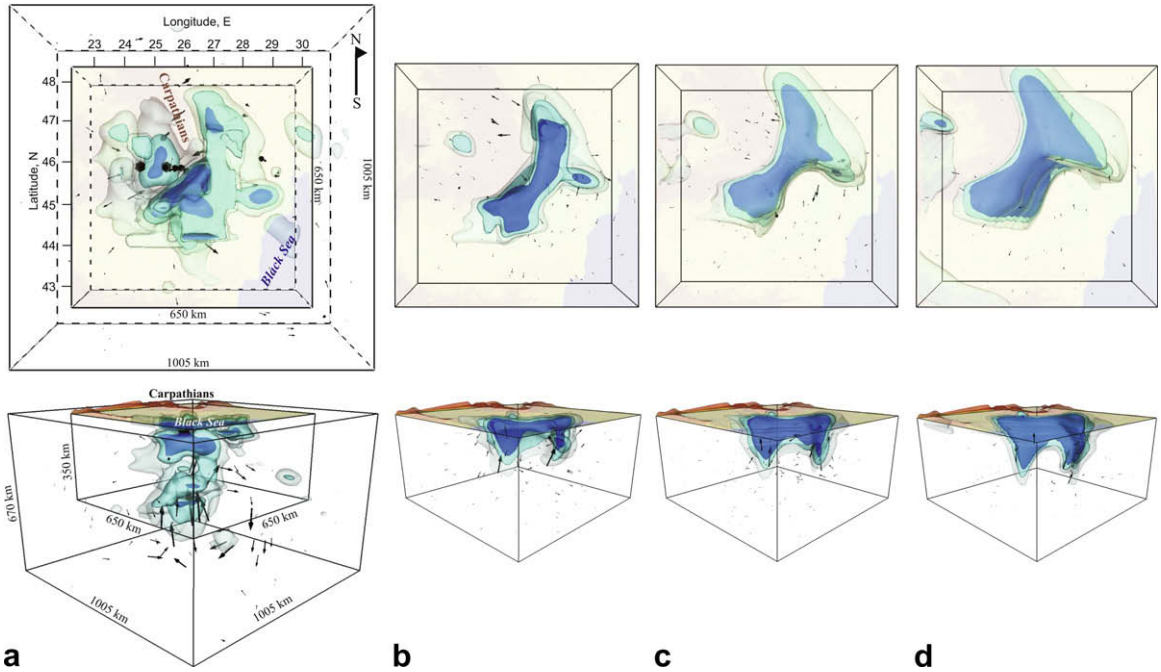

Fig. 2. Model of a descending lithosphere. 3-D thermal shape of the lithospheric slab and contemporary flow induced by the slab descending in the mantle (a). Snapshots of the 3-D thermal shape of the slab and pattern of mantle flow 11 million years ago (b), 16 million years ago (c), and 22 million years ago (d). Upper panel: top view; lower panel: side view from the SE toward NW. Arrows illustrate the direction and magnitude of the flow. The marked sub-domain of the model domain (a) presents the region around the Vrancea shown in b–d. The surfaces marked by blue, dark cyan, and light cyan illustrate the surfaces of 0.07, 0.14, and 0.21 temperature anomaly δT, respectively, where $\delta T = (T_{hav} - T)/T_{hav}$, and T_{hav} is the horizontally averaged temperature. The top surface presents the topography. (For interpretation of the references in color in this figure legend, the reader is referred to the web version of this article.)

Table 1
Comparison of methods for data assimilation in models of mantle dynamics.

	QRV	VAR	BAD
Method	Solving the regularized backward heat problem with respect to parameter β	Iterative sequential solving of the direct and adjoint heat problems	Solving of heat advection equation backward in time
Solution's stability	Stable for parameter β to numerical errors and conditionally stable for parameter β to arbitrarily assigned initial conditions (numerically)	Conditionally stable to numerical errors depending on the number of iterations (theoretically) and unstable to arbitrarily assigned initial conditions (numerically)	Stable theoretically and numerically
Solution's convergence	Numerical solution to the regularized backward heat problem converges to the solution of the backward heat problem in the special class of admissible solutions	Numerical solution converges to the exact solution in the Hilbert space	Not applied
Solution's accuracy	Acceptable accuracy for both synthetic and geophysical data	High accuracy for synthetic data	Low accuracy for both synthetic and geophysical data in conduction-dominated mantle flow
Time interval for data assimilation	Limited by the characteristic thermal diffusion time	Limited by the characteristic thermal diffusion time and the accuracy of the numerical solution	No specific time limitation; depends on mantle flow intensity
Analytical work	Choice of the regularizing operator	Derivation of the adjoint problem	No additional analytical work
Algorithmic work	New solver for the regularized equation should be developed	No new solver should be developed	Solver for the advection equations is to be used

the adjoint problem is identical to the structure of the original problem, which considerably simplifies the numerical implementation. However, the VAR method imposes some requirements for the mathematical model (i.e., a derivation of the adjoint problem). Moreover, for an efficient numerical implementation of the VAR method, the error level of the computations must be adjusted to the parameters of the algorithm, and this complicates computations.

The QRV method allows employing sophisticated mathematical models (because it does not require derivation of an adjoint problem as in the VAR data assimilation) and hence expands the scope for applications in geodynamics (e.g., thermo-chemical convection, phase transformations in the mantle). It does not require that the desired accuracy of computations be directly related to the parameters of the numerical algorithm. However, the regularizing operators usually used in the QRV method enhance the order of the system of differential equations to be solved.

The BAD is the simplest method for data assimilation in models of mantle dynamics, because it does not require any additional work (neither analytical nor computational). The major difference between the BAD method and two other methods (VAR and QRV methods) is that the BAD method is by design expected to work (and hence can be used) only in advection-dominated heat flow. In the regions of high temperature/low mantle viscosity, where

Table 2
Performance of data assimilation methods.

Method	CPU time for one time step (circa, in s)		
	Solving the Stokes problem using $50 \times 50 \times 50$ finite elements	Solving the backward heat problem using $148 \times 148 \times 148$ finite difference mesh	Total
BAD	180	2.5	182.5
QRV	100–180	3	103–183
VAR	360	$1.5n$	$360 + 1.5n$

heat is transferred mainly by convective flow, the use of the BAD method is justified, and the results of numerical reconstructions can be considered to be satisfactory. Otherwise, in the regions of conduction-dominated heat flow (due to either high mantle viscosity or high conductivity of mantle rocks), the use of the BAD method cannot even guarantee any similarity of reconstructed structures. If mantle structures are diffused significantly, the remaining features of the structures can be only backward advected with the flow.

If a thermal feature created, let us say, hundreds million years ago has completely diffused away by the present, it is impossible to restore the feature, which was more prominent in the past. The time to which a present thermal structure in the upper mantle can be restored should be restricted by the characteristic thermal diffusion time, the time when the temperatures of the evolved structure and the ambient mantle are nearly indistinguishable [16]. In fact, the time duration for which data assimilation methods can provide reasonable results is much shorter than the characteristic thermal diffusion time interval. The time interval for the VAR data assimilation depends strongly on smoothness of the input data and the solution. The time interval for the BAD data assimilation depends on the intensity of mantle convection: it is short for conduction-dominated heat transfer and becomes longer for advection-dominated heat flow. We note that in the absence of thermal diffusion the backwards advection of a low-density fluid in the gravity field will finally yield a uniformly stratified, inverted density structure, where the low-density fluid overlain by a dense fluid spreads across the lower boundary of the model domain to form a horizontal layer. Once the layer is formed, information about the evolution of the low-density fluid will be lost, and hence any forward modeling will be useless, because no information on initial conditions will be available.

The QRV method can provide stable results within the characteristic thermal diffusion time interval. However, the length of the time interval for QRV data assimilation depends on several factors. Samarskii and Vabishchevich [36] estimated the temperature misfit between the solution to the backward heat conduction problem and the solution to the regularized backward heat conduction equation and evaluated the time interval $0 \leqslant t \leqslant t_*$ of data assimilation for which the temperature misfit would not exceed a prescribed value. The time duration of data assimilation depends on a regularization parameter, errors in the input data, and smoothness of the temperature function.

Computer performance of the data assimilation methods can be estimated by a comparison of CPU times for solving the inverse problem of thermal convection. Table 2 lists the CPU times required to perform one time-step computations on 16 processors. The CPU time for the case of the QRV method is presented for a given regularization parameter β; in general, the total CPU time increases by a factor of $\Re$, where $\Re$ is the number of runs required to determine the optimal regularization parameter β_*. The numerical solution of the Stokes problem (by the conjugate gradient method) is the most time consuming calculation: it takes about 180 s to reach a high accuracy in computations of the velocity potential. The reduction in the CPU time for the QRV method is attained by employing the velocity potential computed at β_i as an initial guess function for the conjugate gradient method to compute the vector potential at β_{i+1}. An application of the VAR method requires to compute the Stokes problem twice to determine the 'advected' and 'true' velocities [16]. The CPU time required to compute the backward heat problem using the TVD solver is about 3 s in the case of the QRV method and 2.5 s in the case of the BAD method. For the VAR case, the CPU time required to solve the direct and adjoint heat problems by the semi-Lagrangian method is $1.5 \times n$, where n is the number of iterations in the gradient method used to minimize the cost functional (Eq. (8)).

8. Conclusion

Data assimilation methods are useful tools for improving our understanding of the thermal and dynamic evolution of the Earth's structures. We have presented the VAR and QRV methods for data assimilation and their realizations with the aim to restore the evolution of the Earth's thermal structures. We have obtained reasonable scenarios for the evolution of mantle structures since the geological past, which are based on the measurements of the Earth's temperature, heat flux, and surface motions. The basic knowledge we have gained from the case studies is the dynamics of the Earth interior in the past, which could result in its present dynamics.

The VAR and QRV methods have been compared to the BAD method. It is shown that the BAD method can be employed only in models of advection-dominated mantle flow (that is, in the regions where the Rayleigh number is high enough, $>10^7$), whereas the VAR and QRV methods are suitable for the use in models of conduction-dominated flow (lower Rayleigh numbers). The VAR method provides a higher accuracy in restoration of mantle structures compared to the QRV method, but it encounters the problem of increasing noise (without proper smoothing of data and numerical solutions). Meanwhile the QRV method can be applied to assimilate both smooth and non-smooth data. Depending on a geodynamic problem one of the three methods can be employed in solving of inverse retrospective problems of Earth's mantle dynamics.

The present mantle temperature estimated from seismic tomography, the surface movements based on geodetic measurements, and initial and boundary conditions bring uncertainties in data assimilation. The seismic tomography imaging of the Earth and geodetic measurements have their own uncertainties and limitations. The conditions at the boundaries of the model domain used in the data assimilation are, of course, an approximation to the real temperature, heat flux, and movements, which are practically unknown and, what is more important, may change over time at these boundaries. The results of data assimilation will hence depend on the model boundary conditions. Moreover, errors associated with the knowledge of the temperature (or heat flux) evolution or of the regional horizontal surface movements can propagate into the past during data assimilation.

A part of the scientific community may maintain scepticism about the inverse retrospective modeling of thermal evolution of the Earth interior. This scepticism may partly have its roots in our poor knowledge of the Earth's present structure and its physical properties and related uncertainties which cannot allow for rigorous numerical paleoreconstructions of the evolution of Earth's mantle structures. An increase in the accuracy of seismic tomography inversions and geodetic measurements, improvements in the knowledge of gravity and geothermal fields, and more complete experimental data on the physical and chemical properties of

mantle rocks will facilitate reconstructions of thermal structures in the Earth's mantle.

Acknowledgements

This work was supported by the German Research Foundation (DFG), the French Ministry of Research, the Russian Academy of Sciences, and the Russian Foundation for Basic Research. The authors are very grateful to K.-J. Bathe for his insightful comments and suggestions and to the reviewers who provided constructive comments that improved an initial version of the manuscript.

References

[1] Kirsch A. An introduction to the mathematical theory of inverse problems. New York: Springer-Verlag; 1996.
[2] Ismail-Zadeh AT, Talbot CJ, Volozh YA. Dynamic restoration of profiles across diapiric salt structures: numerical approach and its applications. Tectonophysics 2001;337:21–36.
[3] Kaus BJP, Podladchikov YY. Forward and reverse modeling of the three-dimensional viscous Rayleigh–Taylor instability. Geophys Res Lett 2001;28:1095–8.
[4] Korotkii AI, Tsepelev IA, Ismail-Zadeh AT, Naimark BM. Three-dimensional backward modeling in problems of Rayleigh–Taylor instability. Proc Ural State Univ 2002;22(4):96–104.
[5] Ismail-Zadeh AT, Tsepelev IA, Talbot CJ, Korotkii AI. Three-dimensional forward and backward modelling of diapirism: numerical approach and its applicability to the evolution of salt structures in the Pricaspian basin. Tectonophysics 2004;387:81–103.
[6] Steinberger B, O'Connell RJ. Advection of plumes in mantle flow: implications for hotspot motion, mantle viscosity and plume distribution. Geophys J Int 1998;132:412–34.
[7] Conrad CP, Gurnis M. Seismic tomography, surface uplift, and the breakup of Gondwanaland: integrating mantle convection backwards in time. Geochem Geophys Geosyst 2003;4(3). doi:10.1029/2001GC000299.
[8] Bunge H-P, Richards MA, Lithgow-Bertelloni C, Baumgardner JR, Grand SP, Romanowicz B. Time scales and heterogeneous structure in geodynamic earth models. Science 1998;280:91–5.
[9] Bunge H-P, Richards MA, Baumgardner JR. Mantle circulation models with sequential data-assimilation: inferring present-day mantle structure from plate motion histories. Philos Trans R Soc A 2002;360:2545–67.
[10] Kalnay E. Atmospheric modeling, data assimilation and predictability. Cambridge: Cambridge University Press; 2003.
[11] Bennett AF. Inverse methods in physical oceanography. Cambridge: Cambridge University Press; 1992.
[12] McLaughlin D. An integrated approach to hydrologic data assimilation: interpolation, smoothing, and forecasting. Adv Water Resour 2002;25:1275–86.
[13] Bunge HP, Hagelberg CR, Travis BJ. Mantle circulation models with variational data assimilation: inferring past mantle flow and structure from plate motion histories and seismic tomography. Geophys J Int 2003;152:280–301.
[14] Ismail-Zadeh AT, Korotkii AI, Tsepelev IA. Numerical approach to solving problems of slow viscous flow backwards in time. In: Bathe KJ, editor. Computational fluid and solid mechanics. Amsterdam: Elsevier Science; 2003. p. 938–41.
[15] Ismail-Zadeh AT, Korotkii AI, Naimark BM, Tsepelev IA. Three-dimensional numerical simulation of the inverse problem of thermal convection. Comput Math Math Phys 2003;43:587–99.
[16] Ismail-Zadeh A, Schubert G, Tsepelev I, Korotkii A. Inverse problem of thermal convection: numerical approach and application to mantle plume restoration. Phys Earth Planet Inter 2004;145:99–114.
[17] Ismail-Zadeh A, Schubert G, Tsepelev I, Korotkii A. Three-dimensional forward and backward numerical modeling of mantle plume evolution: effects of thermal diffusion. J Geophys Res 2006;111:B06401. doi:10.1029/2005JB003782.
[18] Hier-Majumder CA, Belanger E, DeRosier S, Yuen DA, Vincent AP. Data assimilation for plume models. Nonlinear Process Geophys 2005;12:257–67.
[19] Liu L, Gurnis M. Simultaneous inversion of mantle properties and initial conditions using an adjoint of mantle convection. J Geophys Res 2008;113:B08405. doi:10.1029/2008JB005594.
[20] Lattes R, Lions JL. The method of quasi-reversibility: applications to partial differential equations. New York: Elsevier; 1969.
[21] Ismail-Zadeh A, Korotkii A, Schubert G, Tsepelev I. Quasi-reversibility method for data assimilation in models of mantle dynamics. Geophys J Int 2007;170:1381–98.
[22] Ismail-Zadeh A, Schubert G, Tsepelev I, Korotkii A. Thermal evolution and geometry of the descending lithosphere beneath the SE-Carpathians: an insight from the past. Earth Planet Sci Lett 2008;273:68–79.
[23] Schubert G, Turcotte DL, Olson P. Mantle convection in the Earth and planets. Cambridge: Cambridge University Press; 2001.
[24] Chandrasekhar S. Hydrodynamic and hydromagnetic stability. Oxford: Oxford University Press; 1961.
[25] Boussinesq J. Theorie analytique de la chaleur, vol. 2. Paris: Gauthier-Villars; 1903.
[26] Busse FH, Christensen U, Clever R, Cserepes L, Gable C, Giannandrea E, et al. 3D convection at infinite Prandtl number in Cartesian geometry – a benchmark comparison. Geophys Astrophys Fluid Dynam 1993;75:39–59.
[27] Zou X, Navon IM, Berger M, Phua KH, Schlick T, Le Dimet FX. Numerical experience with limited-memory quasi-Newton and truncated Newton methods. SIAM J Optim 1993;3:582–608.
[28] Daescu DN, Navon IM. An analysis of a hybrid optimization method for variational data assimilation. Int J Comput Fluid Dynam 2003;17:299–306.
[29] Tikhonov AN, Samarskii AA. Equations of mathematical physics. New York: Dover Publications; 1990.
[30] Samarskii AA, Vabishchevich PN, Vasiliev VI. Iterative solution of a retrospective inverse problem of heat conduction. Math Model 1997;9:119–27.
[31] Alekseev AK, Navon IM. The analysis of an ill-posed problem using multiscale resolution and second order adjoint techniques. Comput Method Appl Mech Eng 2001;190:1937–53.
[32] Tikhonov AN, Arsenin VY. Solution of ill-posed problems. Washington, DC: Winston; 1977.
[33] Vernotte P. Les paradoxes de la theorie continue de l'equation de la chaleur. Comptes Rendus 1958;246:3154–5.
[34] Morse PM, Feshbach H. Methods of theoretical physics. New York: McGraw-Hill; 1953.
[35] Cattaneo C. Sur une forme de l'equation de la chaleur elinant le paradox d'une propagation instantance. Comptes Rendus 1958;247:431–3.
[36] Samarskii AA, Vabishchevich PN. Numerical methods for solving inverse problems of mathematical physics. Moscow: URSS; 2004.
[37] Courant R, Isaacson E, Rees M. On the solution of nonlinear hyperbolic differential equations by finite differences. Commun Pure Appl Math 1952;5:243–55.
[38] Staniforth A, Coté J. Semi-Lagrangian integration schemes for atmospheric models – a review. Mon Weather Rev 1991;119(9):2206–23.
[39] Harten A. High resolution schemes for hyperbolic conservation laws. J Comput Phys 1983;49:357–93.
[40] Samarskii AA, Vabishchevich PN. Computational heat transfer. Mathematical modelling, vol. 1. New York: John Wiley and Sons; 1995.
[41] Ismail-Zadeh AT, Korotkii AI, Naimark BM, Tsepelev IA. Numerical modelling of three-dimensional viscous flow under gravity and thermal effects. Comput Math Math Phys 2001;41:1331–45.
[42] Fletcher R, Reeves CM. Function minimization by conjugate gradients. Comput J 1964;7:149–54.
[43] Bathe KJ, Zhang H. A flow-condition-based interpolation finite element procedure for incompressible fluid flows. Comput Struct 2002;80:1267–77.
[44] Kohno H, Bathe KJ. Insight into the flow-condition-based interpolation finite element approach: solution of steady-state advection–diffusion problems. Int J Numer Method Eng 2005;63:197–217.
[45] Ewing RE, Wang H. A summary of numerical methods for time-dependent advection-dominated partial differential equations. J Comput Appl Math 2001;128:423–45.
[46] Wang Y, Hutter K. Comparison of numerical methods with respect to convectively dominated problems. Int J Numer Method Fluid 2001;37:721–45.
[47] Trushkov VV. An example of (3 + 1)-dimensional integrable system. Acta Appl Math 2002;62(1–2):111–22.
[48] Korotkii AI, Tsepelev IA. Solution of a retrospective inverse problem for one nonlinear evolutionary model. Proc Steklov Inst Math 2003;2:80–94.
[49] Davaille A, Vatteville J. On the transient nature of mantle plumes. Geophys Res Lett 2005;32:L14309. doi:10.1029/2005GL023029.
[50] Martin M, Wenzel F. The CALIXTO working group. High-resolution teleseismic body wave tomography beneath SE-Romania – II. Imaging of a slab detachment scenario. Geophys J Int 2006;164:579–95.
[51] Demetrescu C, Andreescu M. On the thermal regime of some tectonic units in a continental collision environment in Romania. Tectonophysics 1994;230:265–76.
[52] Katsura T, Yamada H, Nishikawa O, Song M, Kubo A, Shinmei T, et al. Olivine-wadsleyite transition in the system $(Mg,Fe)_2SiO_4$. J Geophys Res 2004;109:B02209. doi:10.1029/2003JB002438.